Electronic Coupling in Mixed-Valence Binuclear Ruthenium Ammine Complexes As Probed by an Electrochemical Method and an Extension of Mulliken's Theory of Donor–Acceptor Interactions

Faleh Salaymeh, Samson Berhane, Rohana Yusof, Roger de la Rosa, Ella Y. Fung, Regina Matamoros, Kent W. Lau, Qian Zheng, Edward M. Kober,† and Jeff C. Curtis*

Chemistry Department, University of San Francisco, 2130 Fulton Street, San Francisco, California 94117

Received January 7, 1993

An electrochemical approach to assessing the degree of electronic coupling in mixed-valence binuclear complexes is outlined. The method relies on the comparison of electrochemical potential shifts induced at both the *directly* and *indirectly* perturbed metal sites when a ligand substitution process is carried out at one site, e.g., [symmetric] $(NH_3)_5Ru–L_{br}–Ru(NH_3)_5^{4+/5+/6+}$ → [asymmetric] $L(NH_3)_5Ru–L_{br}–Ru(NH_3)_5^{4+/5+/6+}$, where the bridging ligand L_{br} is either pyrazine or 4-cyanopyridine and the perturbing ligand L is a substituted pyridine. It is found that the degree of electronic coupling in these systems is at least three times that which would be predicted based solely on spectroscopic measurements. The stabilization energy due to electron delocalization in these complexes can be accounted for with near-quantitative accuracy. It is also shown how the Mulliken analysis of the data allows for an estimation of the Wolfsberg–Helmholz constant *K*, which can be used in the calculation of off-diagonal matrix elements for molecular donor–acceptor interactions.

The elucidation of the nature and extent of the electronic coupling between redox sites in mixed-valence binuclear complexes continues to offer a challenging fundamental problem. One of the primary frameworks for understanding this area has been the theoretical connection forged by Hush between the electronic coupling and the energy and band shape of an intervalence charge-transfer band in those mixed-valence systems where one is observable.[1,2] In recent work, Reimers and Hush have expanded the approach and applied it to the case of quite weakly coupled systems such as the polyene-bridged Creutz–Taube ion[3] analogues studied by Launay and co-workers.[4,5]

In a previous communication from this laboratory we proposed a new approach to this problem based on a combination of systematic synthetic variations and electrochemical potential measurements.[6] The redox perturbation *directly* induced by ligand substitution at one end of a diruthenium dimer is compared to the perturbation *indirectly* induced at the other end of the dimer. Figure 1 shows an example of the kind of electrochemical measurements used and the quantities of interest. The systems used in the previous study were a series of close synthetic variants of the Creutz–Taube ion,[3]

$$trans\text{-}L(NH_3)_4Ru_b–pz–Ru_a(NH_3)_5^{4+/5+/6+}$$

where pz is pyrazine and L = substituted pyridines of variable $d\pi \rightarrow \pi^*$ back-bonding ability.[7] The ratio of the electrode potential shift at Ru_b (the more positive redox couple) to the shift at Ru_a (the less positive redox couple) upon variation in L at Ru_b was denoted by the variable *m*, and this quantity was related to the degree of mixing between the interacting redox sites using a formalism derived from the Mulliken theory of donor–acceptor interactions.[8,9]

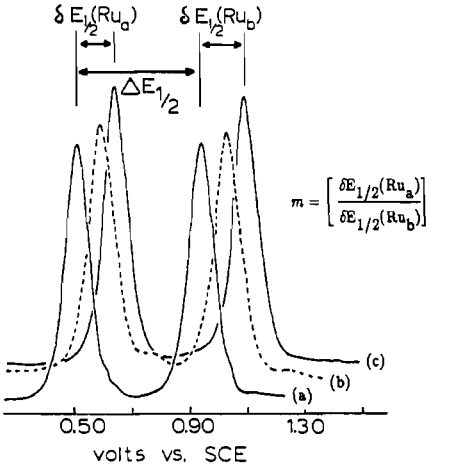

Figure 1. Differential pulse polargrams illustrating potential shifts induced by ligand substitution on the Creutz–Taube ion: (a) $(NH_3)_5Ru–pz–Ru(NH_3)_5^{4+/5+/6+}$; (b) $(NH_3)_5Ru_a–pz–Ru_b(NH_3)_4py^{4+/5+/6+}$; (c) $(NH_3)_5Ru_a–pz–Ru_b(NH_3)_4$2,6-$Me_2Pz^{4+/5+/6+}$.

In the current paper we report on refinements of this approach, application to a broader set of complexes, and comparison with assessments of coupling based on spectroscopic data and the Hush formalism. The complexes used here include series of asymmetrically substituted dimers like the one above but with 4-cyanopyridine (4CP) as bridging ligand as well as symmetrically substituted systems, selected *cis*-substituted dimers, and several rhodium analogs.

Basis of the Hush Formalism. The spectroscopically-based metal–metal coupling formalism developed by Hush[1] arises out of the perturbational treatment of donor–acceptor interactions due to Murrell.[9,10] The potential field of the unreduced acceptor ion is treated as a perturbing term in the Hamiltonian which

† Los Alamos National Laboratory.

(1) (a) Allen, G. C.; Hush, N. S. *Prog. Inorg. Chem.* **1967**, *8*, 357–444. (b) Hush, N. S. *Electrochim. Acta* **1968**, *13*, 1005–1023.
(2) Creutz, C. *Prog. Inorg. Chem.* **1983**, *30*, 1–73.
(3) Creutz, C.; Taube, H. *J. Am. Chem. Soc.* **1973**, *95*, 1086–1094.
(4) (a) Reimers, J. R.; Hush, N. S. *Chem. Phys.* **1989**, *134*, 323–354. (b) Reimers, J. R.; Hush, N. S. *Inorg. Chem.* **1990**, *29*, 3686–3697. (c) Reimers, J. R.; Hush, N. S. *Inorg. Chem.* **1990**, *29*, 4510–4513.
(5) Woitellier, S.; Launay, J. P.; Spangler, C. W. *Inorg. Chem.* **1989**, *28*, 758–762.
(6) De la Rosa, R.; Chang, P. J.; Salaymeh, F.; Curtis, J. C. *Inorg. Chem.* **1985**, *24*, 4229–4231.
(7) The use of substituted pyridines to "tune" the ground and excited electronic properties of ruthenium ammine complexes has been extensively employed by Ford and co-workers: (a) Malouf, G.; Ford, P. C. *J. Am. Chem. Soc.* **1977**, *99*, 7213–7220. (b) Ford, P. C. *Rev. Chem. Intermed.* **1979**, *2*, 267–296. (c) Tfouni, E.; Ford, P. C. *Inorg. Chem.* **1980**, *19*, 72–76.
(8) (a) Mulliken, R. S. *J. Am. Chem. Soc.* **1952**, *64*, 811–824. (b) Mulliken, R. S.; Person, W. B. *Molecular Complexes*; Wiley: New York, 1969. (c) Mulliken, R. S.; Person, W. B. *J. Am. Chem. Soc.* **1969**, *91*, 3409–3413.
(9) Bender, C. J. *Chem. Soc. Rev.* **1986**, *15*, 475–502.

0020-1669/93/1332-3895$04.00/0

operates on the zero-order wave function φ_d describing the system when the exchanging electron is localized completely on the donor ion. The zero-order state with the electron completely localized on the acceptor is designated φ_a. The resulting perturbed wave functions for the ground and excited (charge-transfer) states are written as $\varphi_d' = \varphi_d + \alpha\varphi_a$ and $\varphi_a' = \varphi_a + \lambda\varphi_d$. Murrell derived the perturbational expressions for α and λ as

$$\alpha = \frac{H_{ad} - S_{ad}H_{dd}}{E_d - E_a} \qquad \lambda = \frac{H_{ad} - S_{ad}H_{aa}}{E_a - E_d} \tag{1}$$

where $H_{ad} = \langle\varphi_a|H|\varphi_d\rangle$ and $S_{ad} = \langle\varphi_a/\varphi_d\rangle$. If it is assumed that $|\lambda| \gg |\alpha|$, then the transition dipole between φ_d' and φ_a' is

$$M_{d'a'} = \langle\varphi_d'|\bar{\mu}|\varphi_a'\rangle = \alpha(M_{aa} - M_{dd}) + (M_{da} - S_{ad}M_{dd}) \tag{2a}$$

Hush pointed out that in the limit of small S_{ad} eq 2a reduces to

$$M_{d'a'} \cong e_0\alpha\mathbf{r} \tag{2b}$$

where e_0 is the charge on the electron and r is the distance between the donor and acceptor sites. Since the oscillator strength f can be calculated from experiment as $f = 4.32 \times 10^{-9} \int \epsilon d\nu \cong 4.6 \times 10^{-9}\, \epsilon_{max}\Delta\nu_{1/2}$ (where $\Delta\nu_{1/2}$ is in cm^{-1})[11] and from theory as $f = 1.09 \times 10^{-5}\, (M_{da}/e0)^2\bar{\nu}$ (where the units of M_{da} are electron angstroms),[12] then $|M_{da}| = 0.02(\epsilon(\Delta\nu_{1/2})/\bar{\nu})^{1/2}$ and it follows that

$$\alpha^2 = 4.24 \times 10^{-4}\epsilon_{max}(\Delta\nu_{1/2})/(\bar{\nu}\mathbf{r}^2) \tag{3}$$

where r is in angstroms and $\bar{\nu}$ is typically taken as being ν_{max}.[13] From eq 1 at the $S = 0$ limit it can be seen that the resonance energy due to the charge-transfer interaction in a weakly-coupled system is then

$$H_{ad} = \alpha(E_a - E_d) \cong \alpha\nu_{max} = 2.05 \times 10^{-2}[\epsilon_{max}(\Delta\nu_{1/2})/\nu_{max}]^{1/2}\nu_{max}/\mathbf{r} \tag{4}$$

Equations 3 and 4 have been widely utilized in assessing the degree of electronic coupling between metals in mixed-valence complexes.[1,2,4,5,14-16] One of the most impressive successes of this approach has been the correct prediction of the ordering of intramolecular electron-transfer rates in molecules of the type $(NH_3)_5Co^{III}$–L_{br}–$Ru^{II}(NH_3)_5^{5+}$ based on the couplings calculated from the intervalence-transfer absorption spectra of the corresponding diruthenium species.[17]

Independent experimental confirmation of the quantitative validity of these equations and their range of applicability, however, has been lacking. Recent results indicate that in mixed-valence binuclear copper derivatives of hemocyanin there may be significant disagreement between estimates of the extent of coupling based on eqs 3 and 4 and those based on a detailed analysis of EPR spectral data.[18] Recent investigations by Hupp and co-workers on the metal–ligand coupling in mononuclear complexes of the type $Ru^{II}(NH_3)_4(phen)^{2+}$ and in heteronuclear cyanide-bridged mixed-valence dimers of the type $(NH_3)_5Ru^{III}$–CN–$Fe^{II}(CN)_5^-$ [19,20] also point to stronger coupling than would be indicated by eqs 3 and 4. A very recent report from Hupp's group[21] indicates that application of the Stark spectroscopy results of Oh *et al.*[22] to the symmetrical mixed-valence system $(NH_3)_5Ru^{II}$4,4′–bpy$Ru^{III}(NH_3)_5^{5+}$ might also be consistent with a stronger quantum coupling between the redox sites than previously thought.

The work we report in this article also indicates a divergence from the quantitative estimates arrived at *via* the spectroscopic/perturbational treatment when applied to our relatively strongly coupled systems. The differing effects of *cis vs trans* and symmetric *vs* asymmetric substitution will be discussed. In addition, we will show how the electrochemical/Mulliken approach allows us to account near-quantitatively for the thermodynamic resonance stabilization in these complexes. In the appendix we will show how a straightforward analysis of these systems allows us to evaluate the empirical parameter K of the Wolfsberg–Helmholz relation in the context of molecular donor–acceptor interactions.

Experimental Section

The ruthenium trichloride trihydrate starting material used in this study was provided by the Johnson-Matthey platinum group metals loan program. Rhodium trichloride was purchased from Aesar. Pyrazine "gold label" was purchased from Aldrich and used without further purification, as was ammonium hexafluorophosphate. 4-Cyanopyridine was purchased from Aldrich and recrystallized once from absolute ethanol prior to use. "Omnisolv" acetonitrile was purchased from VWR Scientific and was passed over a column of activated alumina prior to use. The TEA(PF_6) supporting electrolyte used in the electroanalytical experiments was prepared according to the method described by Change *et al.*[23] Tetraethylammonium chloride was purchased from Aldrich and used without further purification.

Starting Materials. $Ru(NH_3)_5Cl(Cl)_2$ was made according to the method described in ref 23. $Ru(NH_3)_5OH_2(PF_6)_2$ was synthesized according to ref 24. The *trans*-substituted compounds *trans*-$LRu(NH_3)_4SO_4(Cl)$ and *trans*-$LRu(NH_3)_4(OH_2)(PF_6)_2$ were synthesized according to ref 23. The starting material for the *cis*-substituted compounds *cis*-$Cl_2Ru(NH_3)_4(Cl)$ was synthesized according to the method of Clarke.[25] Some minor refinements were added to this procedure,[26] and these are outlined below.

***cis*-$[Cl_2Ru^{III}(NH_3)_4]Cl$.** A 5-g amount of $Ru^{III}(NH_3)_5Cl(Cl)_2$ was suspended in 125 mL of argon-degassed concentrated (14.8 M) ammonium hydroxide. The mixture was heated at reflux for approximately 25 min under a blanket of argon until it turned dark pink. At this point 4.95 g of calcium dithionate (Pfaltz-Bauer) was added to the mixture while still hot but not refluxing. The mixture was chilled at 0 °C for 1 h in order to initiate precipitation of the pinkish-white hydroxypentaammineruthenium(III) dithionate. A 200-mL volume of ethanol was added to complete the precipitation of product. The product was isolated by filtration and dried in a vacuum desiccator. The product was then dissolved in 60 mL of argon-degassed, saturated oxalic acid, and the mixture was heated at reflux for no more than 5 min under an argon blanket. At this point a yellow precipitate started to form and the mother liquor turned dark brown. The mixture was chilled at 0 °C for 2 h, and the yellow product, *cis*-(oxalato)tetraammineneuruthenium(III) dithionate, was isolated by filtration and washed with ethanol. The yellow product was then dissolved in 8 M HCl (125 mL), and the solution was heated near reflux for 10 min. After filtration while hot, 125 mL of ethanol was

(10) (a) Murrell, J. N. *J. Am. Chem. Soc.* **1959**, *81*, 5037–5043. (b) Murrell, J. N. *Quart. Rev. (London)* **1961**, *15*, 191–206.
(11) Kauzman, W. *Quantum Mechanics*; Wiley: New York, 1962, p 581 *ff.*
(12) Reference 11, p 644 *ff.* See also: ref 8b, p 25 *ff*; ref 10b, p 197; ref 1a, p 436 *ff.*
(13) This is rigorously true only for Gaussian bands. See: Hush, N. S. *Coord. Chem. Rev.* **1985**, *64*, 135–157.
(14) (a) Richardson, D. E.; Taube, H. *J. Am. Chem. Soc.* **1983**, *105*, 40–51. (b) Richardson, D. E.; Taube, H. *Coord. Chem. Rev.* **1984**, *60*, 107–129.
(15) Aquino, M. A. S.; Bostock, A. E.; Crutchley, R. J. *Inorg. Chem.* **1990**, *29*, 3641–3644.
(16) Kober, E. M.; Goldsby, K. A.; Narayana, D. N. S.; Meyer, T. J. *J. Am. Chem. Soc.* **1983**, *105*, 4303–4309.
(17) (a) Fischer, H.; Tom, G. M.; Taube, H. *J. Am. Chem. Soc.* **1976**, *98*, 5512–5517. (b) Rieder, K.; Taube, H. *Ibid.* **1977**, *99*, 7891–7894. (c) Taube, H. *Ann. Rev. N.Y. Acad. Sci.* **1978**, *313*, 481.
(18) Westmoreland, T. D.; Wilcox, D. E.; Baldwin, M. J.; Mims, W. B.; Solomon, E. I. *J. Am. Chem. Soc.* **1989**, *111*, 6106–6123.
(19) Mines, G. A.; Roberts, J. A.; Hupp, J. T. *Inorg. Chem.* **1992**, *31*, 125–128.
(20) Dong, Y.; Hupp, J. T. *Inorg. Chem.* **1992**, *31*, 3170–3172.
(21) Hupp, J. T.; Dong, Y.; Blackbourn, R. L.; Lu, H. *J. Phys. Chem.* **1993**, *97*, 3278–3282.
(22) (a) Oh, D.; Boxer, S. G. *J. Am. Chem. Soc.* **1990**, *112*, 8161–8162. (b) Oh, D. H.; Sano, M.; Boxer, S. G. *J. Am. Chem. Soc.* **1991**, *113*, 6880–6890.
(23) Chang, P. J.; Fung, E. F.; Curtis, J. C. *Inorg. Chem.* **1986**, *25*, 4233–4241.
(24) Curtis, J. C.; Sullivan, B. P.; Meyer, T. *J. Inorg. Chem.* **1983**, *22*, 224–236.
(25) Clark, R. E. Master's Thesis, Univ. of California at Santa Barbara, 1969.
(26) Berhane, Samson. Master's Thesis, Univ. of San Francisco, 1990.

Table I. Electrochemical Potential Data for the Various Monomeric Species Synthesized in the Course of This Study[a]

L in $L(NH_3)_4RuL_{br}^{2+/3+}$	$E_{1/2}(L_{br}$ = pz) (V)	$E_{1/2}(L_{br}$ = 4CP) (V)
NH_3	0.124 ± 0.003	0.220 ± 0.003
trans-3,5-Me_2py	0.277	0.360
trans-py	0.312	0.396
trans-4-Brpy		0.425
trans-4-Clpy		0.430
trans-3-Clpy	0.357	0.443
trans-3-Fpy	0.375	0.445
trans-2,6-Me_2pz	0.427	0.471
bpy[b]	0.450	0.522
cis-3,5-Me_2py	0.084 ± 0.009	
cis-py	0.310	
cis-3-Fpy	0.340	

[a] All potentials measured vs fc/fc^+ in 0.1 M TEA(PF_6) at a platinum disk electrode. [b] Triammine species.

added to the filtrate and the mixture was cooled overnight at 0 °C. The resulting yellow product, *cis*-$(NH_3)_4RuCl_2(Cl)$, was isolated by filtration and then further purified by recrystallization from warm 8 M HCl/ethanol (≃40 mL of ethanol added to a solution of the product in a minimum volume, ≃30 mL, of 8 M HCl). Chilling at 0 °C for 8 h gave a 65% yield of product. This starting material was found to be long-term stable at room temperature. Subsequent to our own work on this system, a new and reportedly superior synthesis for this starting material was published by Pell et al.[27]

Asymmetrically *Trans*-Substituted Dimers. The dimers *trans*-$L(NH_3)_4Ru^{II}$–L_{br}–$Ru^{II}(NH_3)_5(PF_6)_4$, where L_{br} = pyrazine (pz) or 4-cyanopyridine (4CP), were synthesized in a two-step procedure. The first step was the synthesis of the appropriate monomeric starting compound as described below.

Monomers. *trans*-$LRu(NH_3)_4L_{br}(PF_6)_2$. In the case where L_{br} = pyrazine, the required monomeric units were synthesized by reacting about 100 mg of the *trans*-$LRu(NH_3)_4(OH_2)(PF_6)_2$ starting material with a 2- or 3-fold molar excess of pz in 20 mL of argon-degassed acetone at room temperature for 2 h. This solution was filtered into a 5-fold volume of stirring ether in order to precipitate the monomeric product. Yields were 80% to 60% depending on the purity of the initial *trans*-$LRu(OH_2)$ starting material. In the case where L_{br} was the 4-cyanopyridine ligand, syntheses were performed using the starting material *trans*-$L(NH_3)_4Ru^{III}(SO_4)Cl$ and a method similar to that outlined by Clarke and Ford[28] and by Katz *et al.*[29] The sulfato complex (about 100 mg) was reduced over Zn/Hg amalgam in water (about 3 mL) at about pH 3 (addition of a small amount or trifluoroacetic acid vapor was frequently used to attain this condition). The resulting solution of *trans*-$LRu(NH_3)_4(H_2O)^{2+}$ was added slowly to a stirring, argon-degassed solution of a 6-fold excess of 4-cyanopyridine. After 1 h of reaction at room temperature, excess NH_4PF_6 was added and the resulting *trans*-$LRu(NH_3)_4$4CP$(PF_6)_2$ solid was isolated by filtration. The major product (*ca.* 90%) from this reaction is the nitrile-bound isomer,[30] but in some cases there was a small low-potential shoulder in the differential pulse polarograms which probably corresponded to the pyridine-bound minority product which is known to form under these conditions.[29] This impurity could be removed by slow, partial reprecipitation of the complex (with some sacrifice in yield) from concentrated acetone solution by slow addition of diethyl ether or toluene at 0 °C.[23] Electrochemical potential data for the monomeric ruthenium species synthesized in the course of this study are listed in Table I.

Dimers. The asymmetric dimeric species were then made by reacting 60–90 mg of the *trans*-$LRuL_{br}$ monomeric species with a 3-fold molar excess of $(NH_3)_5Ru(OH_2)(PF_6)_2$ in 20 mL of argon-degassed acetone at 40–50 °C for 24 h. The crude product was isolated by filtering this solution into five volumes of ether. The oxo-bridged $((NH_3)_5Ru)_2O(PF_6)_4$ impurity which forms due to excess pentaammine aquo can be eliminated by metathesis to the chloride using a nearly saturated solution of tetraethylammonium chloride (TEACl) in 70:30 acetone/methanol followed by isolation of the PF_6^- salt from water using ammonium hexafluorophosphate as described in ref 23. Yields of pure dimer were typically on the order of 50–70% except for the case for L = 2,6-Me_2pz, which was only 20% due to the relatively high solubility of the PF_6^- salt in water. Before electrochemical or elemental analysis it is important to isolate the final dimeric product at least once from acetone/stirring ether in order to eliminate any excess NH_4PF_6. In some cases electrochemical analysis by differential pulse polarography will show the presence of some unreacted *trans*-$LRuL_{br}$ starting material. This can be eliminated by partial reprecipitation from acetone/ether or acetone/toluene as described in ref 23. This procedure diminishes the final yield, however; thus it is preferable to avoid its necessity by being to sure to use fairly fresh pentaammine aquo (less than 2-weeks old) in sufficient excess and according to the above conditions so that the dimerization goes to completion. Purity of the final product could be readily assessed by differential pulse polarography. The presence two and only two peaks of equal heights (within 10%) was taken as evidence for a pure(or at least monomer-free) dimer. Elemental analysis results for those compounds analyzed are summarized in Table II. Electroanalytical and near-IR spectroscopic data for the asymmetric pyrazine-bridged dimers are summarized in Table III. Data for the asymmetric 4-cyanopyridine dimers are in Table IV.

Symmetrical *trans*-Substituted Dimers. Dimers of the general formula (*trans*-$LRu(NH_3)_4)_2L_{br}(PF_6)_4$ were synthesized by reacting 100–120 mg of the appropriate *trans*-$LRu(OH_2)$ starting compound[23] with 0.3 equiv of L_{br} (pyrazine or 4-cyanopyridine) in 20 mL of argon-degassed acetone at 40–50 °C for 24 h. Workup proceeded as described above. Elemental analysis results for those compounds analyzed are shown in Table II. Electroanalytical and spectroscopic data are summarized in Table V for the pz-bridged series and in Table VI for the 4CP-bridged series.

Asymmetrical *Cis*-Substituted Dimers. *cis*-$L(NH_3)_4Ru^{II}pzRu^{II}(NH_3)_5(PF_6)_4$. The first step in these syntheses was to make the appropriate monomeric units, *cis*-$L(NH_3)_4Ru^{II}pz(PF_6)_2$.

Monomers. *cis*-$L(NH_3)_4Ru^{II}pz(PF_6)_2$. These species were made via the *cis*-$L(NH_3)_4Ru^{III}Cl(Cl)_2$ intermediate described by Marchant *et al.*[31] and also employed by Pavanin *et al.*[32] In a typical preparation, 0.200 g of the *cis*-$[Cl_2(NH_3)_4Ru^{III}]Cl$ starting material (0.726 mmol) was reduced over Zn/Hg amalgam in 5 mL of argon-degassed H_2O. After about 5 min of reduction, an argon-degassed solution of 52 mg of pyridine (0.658 mmol) in 1.5 mL of degassed water was slowly added dropwise with stirring over a period of 10 min (entire solution still over the amalgam). The reaction was allowed to continue for another 20–30 min, at which time the amalgam was filtered away and resulting solution of *cis*-py$(NH_3)_4Ru^{II}(OH_2)^{2+}$ was oxidized to the *cis*-py$(NH_3)Ru^{III}Cl^{3+}$ by the dropwise addition of a 1:1 mixture of 2 M HCl and 30% H_2O_2. Oxidation was judged to be complete when the solution had changed from the orange-brown color of the Ru(II) species to the pale yellow characteristic of the Ru(III). The dichloride salt, *cis*-py$(NH_3)_4Ru^{III}Cl(Cl)_2$, was then precipitated in near-quantitative yield by the addition of 15 volumes of acetone. This product is long-term stable as a solid.

Reduction of this product over Zn/Hg amalgam in argon-degassed H_2O leads to the regeneration of the Ru(II) aquo compound in reasonable purity. Dropwise addition of a solution of the *cis*-py$(NH_3)_4Ru^{II}(OH_2)^{2+}$ generated in this manner to a stirring, argon-degassed solution of a 6-fold excess of pyrazine leads rapidly to the desired *cis*-py$(NH_3)_4Ru^{II}pz^{2+}$ product. This product can then be isolated as the PF_6^- salt via the addition of a large excess of NH_4PF_6. Several reprecipitations from acetone/ether should be performed in order to eliminate excess NH_4PF_6. Yields for this step were on the order of 65% for L = pyridine and 50% for L = 3-fluoropyridine.

Dimers. The asymmetrical dimers *cis*-$L(NH_3)_4Ru^{II}pzRu^{II}(NH_3)_5(PF_6)_4$ were readily synthesized by capping the monomer with $Ru^{II}(NH_3)_5(OH_2)^{2+}$ in degassed acetone as described above for the analogous *trans*-substituted asymmetrical species.

Symmetrical *Cis*-Substituted Dimers. [(*cis*-$L(NH_3)_4Ru^{II})_2pz](PF_6)_4$. These complexes were synthesized in acetone using *cis*-$L(NH_3)_4Ru^{II}(OH_2)(PF_6)_2$ monomer isolated from a freshly reduced aqueous solution of the appropriate ruthenium(III) trichloride complex prepared according to the method described above. In a typical preparation, 150 mg of the *cis*-py$(NH_3)_4Ru(OH_2)(PF_6)_2$ starting material was reacted in argon-degassed acetone with 5.4 mg (0.25 equiv) of pyrazine bridging ligand. After 24 h at 40 °C, the resulting purple-red solution was filtered and

(27) Pell, S. D.; Sherban, M. M.; Tramontano, V.; Clarke, M. J. *Inorg. Synth.* **1989**, *26*, 65–68.
(28) Clarke, R. E.; Ford, P. C. *Inorg. Chem.* **1970**, *9*, 495–499. (See also ref 27.)
(29) Katz, N. E.; Creutz, C.; Sutin, N. *Inorg. Chem.* **1988**, *27*, 1687–1694.
(30) Allen, R. J.; Ford, P. C. *Inorg. Chem.* **1972**, *11*, 679–685.
(31) Marchant, J. A.; Matsubara, T.; Ford, P. C. *Inorg. Chem.* **1977**, *16*, 2160–2165.
(32) Pavanin, L. A.; Giesbrecht, E.; Tfouni, E. *Inorg. Chem.* **1985**, *24*, 4444–4446.

Table II. Elemental Analytical Data (%) for a Sampling of the Compounds Used in This Study

compd	C: obs (theor)	H: obs (theor)	N: obs (theor)	C/N: obs (theor)
trans-3FpyA$_4$Ru(4CP)RuA$_5$(PF$_6$)$_4$·2CH$_3$COCH$_3$	15.87 (16.29)	3.84 (3.78)	13.21 (13.47)	1.20 (1.21)
trans-3,5Me$_2$pyA$_4$Ru(4CP)RuA$_5$(PF$_6$)$_4$·CH$_3$COCH$_3$	15.89 (15.94)	3.92 (3.85)	13.88 (14.01)	1.14 (1.14)
trans-pyA$_4$Ru(4CP)RuA$_5$(PF$_6$)$_4$·2H$_2$O	10.93 (11.44)	3.21 (3.49)	14.13 (14.61)	0.77 (0.78)
(*cis*-pyA$_4$Ru)$_2$pz(PF$_6$)$_4$	15.24 (14.54)	3.76 (3.31)	13.94 (14.53)	1.09 (1.00)
(*cis*-3FpyA$_4$Ru)$_2$pz(PF$_6$)$_4$·CH$_3$COCH$_3$	15.55 (16.32)	3.71 (3.39)	13.38 (13.44)	1.16 (1.21)
trans-pyA$_4$Ru(4CP)RhA$_5$(ClO$_4$)$_5$·2H$_2$O	10.32 (10.28)	3.63 (3.83)	15.60 (16.06)	0.66 (0.64)
A$_5$Ru(4CP)RhA$_5$(ClO$_4$)$_5$·H$_2$O	7.44 (7.24)	3.61 (3.65)	16.86 (16.96)	0.44 (0.43)

Table III. Electrochemical and Spectroscopic Data for the Asymmetrical Pyrazine-Bridged Dimers *trans*-L(NH$_3$)$_4$Ru$_b$pzRu$_a$(NH$_3$)$_5$(PF$_6$)$_4$, Rhodium Analogues *trans*-L(NH$_3$)$_4$Ru$_6$pzRh(NH$_3$)$_5$(PF$_6$)$_5$, and the Dimers *cis*-L(NH$_3$)$_4$Ru$_b$pzRu$_a$(NH$_3$)$_5$(PF$_6$)$_4$

L	$E_{1/2}$(Ru$_a$)	$E_{1/2}$(Ru$_b$)	$\Delta E_{1/2}$[a]	$\delta E_{1/2}$(Ru$_a$)[b]	$\delta E_{1/2}$(Ru$_b$)[c]	m[d]	E_{op} (nm)	E_{op} (eV)	ϵ_{max}	$\Delta\nu_{1/2}$ (eV)
				trans-L(NH$_3$)$_4$RubpzRua(NH$_3$)$_5$(PF$_6$)$_4$						
(1) NH$_3$	0.042[e]	0.473	0.431				1596	0.777	7620	0.184
(2) 3,5-Me$_2$py	0.117	0.536	0.419	0.075	0.063	1.19	1624	0.763	4300	0.246
(3) py	0.128	0.563	0.435	0.086	0.090	0.96	1595	0.777	3050	0.300
(4) 3-Fpy	0.134	0.601	0.467	0.092	0.128	0.72	1500	0.827	2420	0.409
(5) 3-Clpy	0.146	0.602	0.456	0.104	0.129	0.81	1488	0.833	3400	0.389
(6) 2,6-Me$_2$pz	0.167	0.620	0.453	0.125	0.147	0.85	1345	0.922	2430	0.478
(7) bpy[f]	0.189	0.643	0.454	0.147	0.170	0.87	1153	1.075	1650	0.510
						0.90[g]				
				cis-L(NH$_3$)$_4$Ru$_b$pzRu$_a$(NH$_3$)$_5$(PF$_6$)$_4$						
(1) 3,5-Me$_2$py	0.015	0.440	0.425	–0.027	–0.033	0.82	1597	0.776	4160	0.218
(2) py	0.099	0.589	0.490	0.057	0.116	0.49	1441	0.861	2920	0.392
(3) 3-Fpy	0.104	0.609	0.505	0.062	0.136	0.46	1541	0.805	2790	0.418

[a] $\Delta E_{1/2} \equiv E_{1/2}(Ru_b) - E_{1/2}(Ru_a)$. [b] $\delta E_{1/2}(Ru_a) \equiv E_{1/2}(Ru_a)(LA_4Ru_bpzRu_aA_5^{4+/5+}) - E_{1/2}(Ru_a)(A_5Ru_bpzRu_aA_5^{4+/5+})$. [c] $\delta E_{1/2}(Ru_b) \equiv E_{1/2}(Ru_b)(LA_4Ru_bpzRu_aA_5^{5+/6+}) - E_{1/2}(Ru_b)(A_5Ru_bpzRu_aA_5^{5+/6+})$. [d] $m \equiv \delta E_{1/2}(Ru_a)/\delta E_{1/2}(Ru_b)$. [e] All potentials measured in acetonitrile/0.1 M TEA(PF$_6$) *vs* fc/fc$^+$. [f] Triammine species. [g] Average value.

Table IV. Electrochemical and Spectroscopic Data for the Symmetrical Pyrazine-Bridged Dimers *trans*-(L(NH$_3$)$_4$Ru($_2$pz(PF$_6$)$_4$ and *cis*-(L(NH$_3$)$_4$Ru)$_2$pz(PF$_6$)$_4$ and the Rhodium Analogues *trans*-L(NH$_3$)$_4$RupzRh(NH$_3$)$_5$(PF$_6$)$_5$

L	$E_{1/2}$(Ru$_a$)	$E_{1/2}$(Ru$_b$)	$\Delta E_{1/2}$[a]	$\delta' E_{1/2}$(Ru$_a$)[b]	$\delta' E_{1/2}$(Ru$_b$)[c]	m'[d]	E_{op} (nm)	E_{op} (eV)	ϵ_{max}	$\Delta\nu_{1/2}$ (eV)
				trans-(L(NH$_3$)$_4$Ru)$_2$pz(PF$_6$)$_4$						
(1) NH$_3$	0.042[e]	0.473	0.431				1596	0.777	7620	0.184
(2) 3,5-Me$_2$py	0.220	0.575	0.355	0.103	0.039	0.38	1703	0.728	3040	0.244
(3) py	0.242	0.582	0.340	0.114	0.019	0.17	1685	0.736	5940	0.229
(4) 3-Fpy	0.347	0.669	0.305	0.213	0.068	0.32	1690	0.734	9100	0.240
(5) 3-Clpy	0.351	0.672	0.321	0.205	0.070	0.34	1692	0.732	4360	0.241
(6) 2,6-Me$_2$pz	0.376	0.656	0.280	0.209	0.036	0.17	1690	0.730	1525	0.410
(7) bpy[f]	0.444	0.674	0.230	0.255	0.031	0.12	1140	0.861	920	0.497
						0.25[g]				
				trans-(L(NH$_3$)RupzRh(NH$_3$)$_4$(PF$_6$)$_5$						
(1) NH$_3$		0.392			–0.081					
(2) py		0.533			–0.049					
(3) 3-Clpy		0.564			–0.108					
(4) 3-Fpy		0.512			–0.157					
				cis-(L(NH$_3$)$_4$Ru)$_2$pz(PF$_6$)$_5$						
(1) py	0.260	0.628	0.368	0.161	0.039	0.24	1648	0.752	6000	0.220
(2) 3-Fpy	0.336	0.699	0.363	0.232	0.090	0.39	1651	0.751	4570	0.222
						0.32[g]				

[a] $\Delta E_{1/2} \equiv E_{1/2}(Ru_b) - E_{1/2}(Ru_a)$. [b] $\delta' E_{1/2}(Ru_a) \equiv E_{1/2}(Ru_a)((LA_4Ru)_2pz^{4+/5+}) - E_{1/2}(Ru_a)(LA_4Ru_bpzRu_aA_5^{4+/5+})$. [c] $\delta' E_{1/2}(Ru_b) \equiv E_{1/2}(Ru_b)-((LA_4Ru)_2pz^{5+/6+}) - E_{1/2}(Ru_b)(LA_4Ru_b)(LA_4Ru_bpzRu_aA_5^{5+/6+})$. [d] $m' \equiv (\delta' E_{1/2}(Ru_b)/(\delta' E_{1/2}(Ru_a))$. [e] All potentials measured in acetonitrile/0.1 M TEA(PF$_6$) *vs* fc/fc$^+$. [f] Triammine species. [g] Average value.

the crude product was precipitated as the chloride salt by the dropwise addition of a nearly saturated solution of TEACl in 70:30 acetone/methanol (care must be taken not to add more than what is necessary to completely precipitate the dimer). After several washings with acetone, the crude chloride salt was briefly dried by suction in air and then precipitated from water (after filtration) as the PF_6^- by the addition of NH_4PF_6. Purification of these molecules proved to be rather difficult. It was finally found that unreacted monomeric impurities could be removed by *partially* precipitating the chloride salt of the dimer from an acetone solution of the PF_6^- salt using a fairly dilute (about one-fourth saturated) solution of TEACl in acetone/methanol. The desired dimeric product comes out of acetone before the monomeric impurity under these conditions. Final purification was achieved by several reprecipitations from acetone using a large excess (five volumes) of ether to force the product out. Microanalytical data for the compounds analyzed are in Table II.

Rhodium/Ruthenium Analogs of the *Trans*-Substituted Dimers. The rhodium analogues of a selection of the *trans*-substituted diruthenium dimers were made from the appropriate rhodium monomeric species, $(NH_3)_5Rh^{III}L(ClO_4)_3$.

Rhodium Monomers. The starting material for these monomers was the aquo compound $(NH_3)_5Rh(H_2O)(ClO_4)_3$ synthesized by the method of Foust and Ford[33] from rhodium(III) pentaammine trichloride (Aesar). The substituted pentammine species, $(NH_3)_5Rh^{III}L(ClO_4)_3$, were then made using the method of Pfenning *et al.*[34] Gelroth *et al.* report that the pyridine-bound product predominates with 4-cyanopyridine as entering ligand on Rh(III).[35] This fact was confirmed by FTIR experiments which showed that the nitrile stretch of the $(NH_3)_5Rh4CP(ClO_4)_3$ is at 2238 cm^{-1}—very close to the frequency for the free ligand at 2243 cm^{-1}.[36]

(33) Foust, R. D.; Ford, P. C. *Inorg. Chem.* **1972**, *11*, 899–890.
(34) Pfenning, K. J.; Lee, L.; Wholers, H. D.; Petersen, J. D. *Inorg. Chem.* **1982**, *21*, 2477–2482.
(35) Gelroth, J. A.; Figard, J. E.; Petersen, J. D. *J. Am. Chem. Soc.* **1979**, *101*, 3649.
(36) Curtin, E. H.; Katz, N. E. *Polyhedron* **1987**, *6*, 159–162.

Table V. Electrochemical and Spectroscopic Data for the Asymmetrical 4-Cyanopyridine-Bridged Dimers *trans*-$L(NH_3)_4Ru_b{}^4CPRu_a(NH_3)_5(PF_6)_4$

L	$E_{1/2}(Ru_a)$	$E_{1/2}(Ru_b)$	$\Delta E_{1/2}{}^a$	$\delta E_{1/2}(Ru_a)^b$	$\delta E_{1/2}(Ru_b)^c$	m^d	E_{op} (nm)	E_{op} (eV)	ϵ_{max}	$\Delta\nu_{1/2}$ (eV)
(1) NH_3	0.056[e]	0.331	0.275				1020	1.216	1275	0.618
(2) 3,5-Me_2py	0.069	0.430	0.361	0.013	0.099	0.13	908	1.370	1010	0.658
(3) py	0.079	0.466	0.387	0.023	0.135	0.17	892	1.390	1145	0.608
(4) 4-Clpy	0.076	0.494	0.418	0.020	0.163	0.12	860	1.442	560	0.641
(5) 4-Brpy	0.077	0.499	0.422	0.021	0.168	0.13	873	1.420	480	0.655
(6) 3-Clpy	0.089	0.524	0.435	0.033	0.193	0.17	860	1.442	1000	0.660
(7) 3-Fpy	0.088	0.513	0.425	0.032	0.182	0.18	850	1.459	940	0.655
(8) 2,6-Me_2pz	0.079	0.534	0.455	0.023	0.203	0.11	840	1.476	660	0.672
						0.14[f]				

[a] $\Delta E_{1/2} = E_{1/2}(Ru_b) - E_{1/2}(Ru_a)$. [b] $\delta E_{1/2}(Ru_a) \equiv E_{1/2}(Ru_a)(LA_4Ru_b4CPRu_aA_5{}^{4+/5+}) - E_{1/2}(Ru_a)(A_5Ru_b4CPRu_aA_5{}^{4+/5+})$. [c] $\delta E_{1/2}(Ru_b) \equiv E_{1/2}(Ru_b)(LA_4Ru_b4CPRu_aA_5{}^{5+/6+}) - E_{1/2}(Ru_b)(A_5Ru_b4CPRu_aA_5{}^{5+/6+})$. [d] $m \equiv (\delta E_{1/2}(Ru_a))/\delta E_{1/2}(Ru_b))$. [e] All potentials measured in acetonitrile/0.1 M TEA(PF_6) *vs* fc/fc$^+$. [f] Average value.

Table VI. Electrochemical and Spectroscopic Data for the Symmetrical 4-Cyanopyridine-Bridged Dimers *trans*-$(L(NH_3)_4Ru)_24CP(PF_6)_4$ and the Rhodium Analogues *trans*-$L(NH_3)_4Ru4CPRh(NH_3)_5(PF_6)_5$

L	$E_{1/2}(Ru_a)$	$E_{1/2}(Ru_b)$	$\Delta E_{1/2}{}^a$	$\delta' E_{1/2}(Ru_a)^b$	$\delta' E_{1/2}(Ru_b)^c$	$m'{}^d$	E_{op} (nm)	E_{op} (eV)	ϵ_{max}	$\Delta\nu_{1/2}$ (eV)
				trans-$(L(NH_3)_4Ru)_24CP(PF_6)_4$						
(1) NH_3	0.056[e]	0.331	0.275				1020	1.216	1280	0.663
(2) 3,5-Me_2py	0.220	0.437	0.217	0.151	0.007	0.046	1026	1.209	890	0.712
(3) py	0.250	0.475	0.225	0.171	0.009	0.053	1028	1.206	1580	0.600
(5) 4-Brpy	0.295	0.515	0.220	0.218	0.016	0.073	1050	1.181	1780	0.602
(4) 4-Clpy	0.295	0.512	0.217	0.219	0.018	0.082	1042	1.190	1480	0.629
(6) 3-Clpy	0.308	0.525	0.217	0.219	0.001	0.005(?)	1035	1.200	1080	0.630
(7) 3-Fpy	0.310	0.526	0.216	0.222	0.013	0.059	1033	1.201	940	0.620
(8) 2,6-Me_2pz	0.335	0.545	0.210	0.256	0.011	0.043	960	1.290	450	0.750
(9) bpy[f]	0.399	0.575	0.176				994	1.248	660	0.740
						0.052[g]				
				trans-$L(NH_3)_4Ru4CPRh(NH_3)_4(PF_6)_5$						
(1) NH_3		0.306			−0.025					
(2) py		0.462			−0.013					
(3) 3-Clpy		0.504			−0.021					
(4) 4-Brpy		0.492			−0.023					

[a] $\Delta E_{1/2} \equiv E_{1/2}(Ru_b) - E_{1/2}(Ru_a)$. [b] $\delta' E_{1/2}(Ru_a) \equiv E_{1/2}(Ru_a)((tr\text{-}LA_4Ru)_24CP^{4+/5+}) - E_{1/2}(Ru_a)(tr\text{-}LA_4Ru_b4CPRu_aA_5{}^{4+/5+})$. [c] $\delta' E_{1/2}(Ru_b) \equiv E_{1/2}(Ru_b)((LA_4Ru)_24CP^{5+/6+}) - E_{1/2}(Ru_b)(tr\text{-}LA_4Ru_b4CPRu_aA_5{}^{5+/6+})$. [d] $m' \equiv (\delta' E_{1/2}(Ru_b))/(\delta' E_{1/2}(Ru_a))$. [e] All potentials measured in acetonitrile/0.1 M TEA(PF_6) *vs* fc/fc$^+$. [f] Triammine species. [g] Average value.

Coordination at the nitrile functionaliy would be expected to give a positive 50–60 cm^{-1} shift.[33]

Dimers. The dimers *trans*-$L(NH_3)_4RuL_{br}Rh(NH_3)_5(ClO_4)_5$ were then synthesized in degassed water by reacting the rhodium pentaammine species with the appropriate *trans*-$L(NH_3)_4Ru(OH_2)^{2+}$ compound (prepared as described in ref 23). The perchlorate anions from the rhodium pentaammine (L) would interfere with the dimerization step; hence, it was necessary to first exchange them with chlorides via anion exchange on Dowex 1-X4 anion-exchange resin. The resulting solution of $(NH_3)_5Rh^{III}L_{br}(Cl)_3$ (typically starting from 120 mg of the perchlorate, now in a total solution volume of 4–5 mL) was degassed with Ar and then reacted with a 30% molar excess of the freshly prepared ruthenium aquo compound in 3–4 mL of water for 36 h at 40 °C. The crude dimeric product was then precipitated by addition of a large excess of $LiClO_4$. Yields were on the order of 40–50%. In some cases precipitation was enhanced by the addition of up to one volume of *tert*-butyl alcohol. The crude products could be recrystallized from dilute, aqueous perchlorate.

Caution! Perchlorate salts are explosive and should be handled with great care. Quantities in excess of 30–40 mg should not be isolated; vacuum dessiccation to extreme dryness should be avoided. Samples should always be looked upon as a potential source of ignition with respect to flammable organics.

It was found that conversion to the PF_6^- salts of these dimers was necessary in order to obtain reasonable solubility in our electrochemical solvent (acetonitrile/0.1 M TEA(PF_6)). Metathesis was accomplished by dissolving the perchlorate salt in a minimum of warm water and then adding a large excess of NH_4PF_6 and chilling the solution of 0 °C. In some cases it was again necessary to enhance precipitation with small amounts of *tert*-butyl alcohol. In cases where mixed ClO_4^-/PF_6^- salts were obtained, the pure PF_6^- could be isolated by dissolving product in an acetone/water mixture containing excess NH_4PF_6 and then evaporating the acetone on a rotary evaporator. Overall yields were on the order of 20–30%. Microanalytical data are listed in Table II; electroanalytical data are in Tables III and VI. The nature of the linkage isomer for 4CP as a bridge was confirmed as being $Ru^{II}NCpyRh^{III}$ by FTIR. Upon reaction of the $Ru^{III}4CP$ monomer with $(NH_3)_5Ru^{II}(OH_2)^{2+}$ for example, the nitrile stretch shifted from 2238 to 2195 cm^{-1}—a position consistent with nitrile coordinated to ruthenium(II).[28]

Electrochemical Measurements. Differential pulse polarography was used to assess compound purity and to determine $E_{1/2}$ values. An IBM 225 volatmmetric analyzer was used in all measurements. The working electrode was in all cases a freshly polished a platinum disk, and the reference electrode was a saturated KCl calomel electrode. It was found that the day-to-day drift of the calomel electrode was sufficient to obscure the small potential differences being probed in this investigation. Hence it was found to be necessary to calibrate the reference against the ferrocene/ferrocenium couple with each and every potential determination. All potentials listed in this work are referenced directly to the fc/fc$^+$ couple. The supporting electrolyte was in all cases 0.1 M tetraethylammonium hexafluorophosphate (TEAH) synthesized as in ref 23. Standard DPP parameters were 2.0 mV/s scan rate, 15-mV pulse amplitude, 0.1 drop time, and 0.1-s time constant.

Near-Infrared Spectra. Spectra were recorded on a Perkin-Elmer 330 UV–vis–near-IR spectrophotometer. The oxidant used to generate the II,III mixed-valence species *in situ* from the II,II dimers was $Fe(bpy)_3(PF_6)_3$ (prepared according to the method described in ref 23). In a typical experiment, the oxidant was added in small increments (about 0.2 equiv) until the intervalence-transfer band maximum was observed to rise and then begin to fall. The absorbance and peak position for the most strongly absorbing trace was taken as being representative of the pure II,III dimer. The dimers investigated in this study all have sufficiently large $\Delta E_{1/2}$ values (difference between first and second reduction potentials) that corrections for comproportionation to the observed extinction coefficients were ignored.[37]

FTIR Spectra. FTIR spectra were recorded on a Nicolet DX20B spectrometer using pressed KBr pellets to contain the sample.

(37) (a) Sutton, J. E.; Sutton, P. M.; Taube, H. *Inorg. Chem.* **1979**, *18*, 1017–1021. (b) Sutton, J. E.; Taube, H. *Inorg. Chem.* **1981**, *20*, 3125–3134.

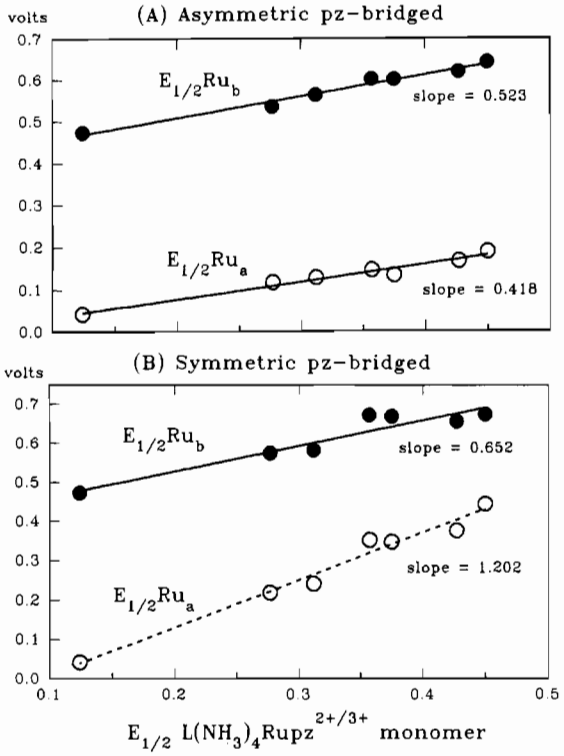

Figure 2. $E_{1/2}(Ru_a)$ and $E_{1/2}(Ru_b)$ for the pz-bridged dimers vs $E_{1/2}$ for the appropriate monomeric species *trans*-$LA_4Rupz^{2+/3+}$ (data from in Tables I, III, and IV).

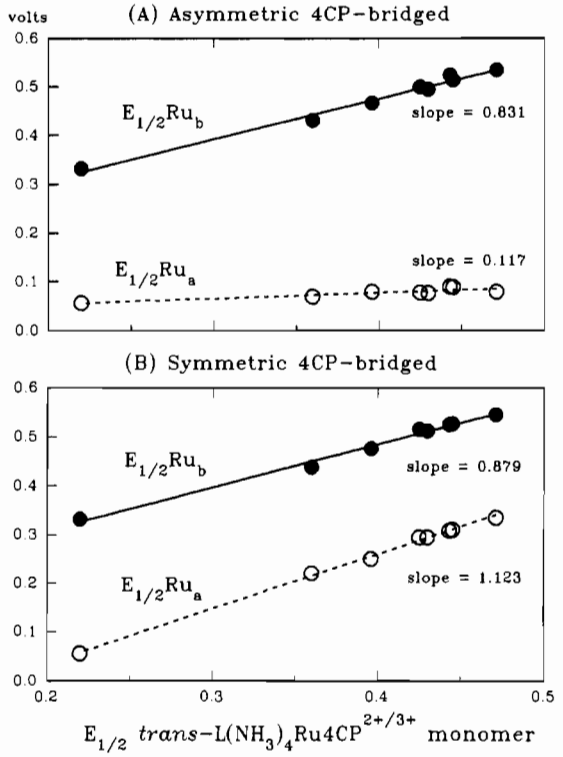

Figure 3. $E_{1/2}(Ru_a)$ and $E_{1/2}(Ru_b)$ for the 4CP-bridged dimers vs $E_{1/2}$ for the appropriate monomeric species *trans*-$LA_4Ru4CP^{2+/3+}$ (data from Tables I, V, and VI).

Results and Discussion

The electrochemical and near-IR spectroscopic data for the various dimers investigated are shown in Tables III–VI. From Table III, for example, we see that upon going from *trans*-L = NH_3 (entry number one, the Creutz–Taube ion) to *trans*-L = py in the asymmetric, *trans*-substituted series that the redox potential of the directly perturbed metal, Ru_b, shifts by 0.090 V while that of the indirectly perturbed metal, Ru_a, shifts by 0.086 V. The ratio of these shifts as defined by $m \equiv (\delta E_{1/2}(Ru_a))/(\delta E_{1/2}(Ru_b))$ is then 0.96. Further inspection of this table shows that if the perturbing pyridine ligand is attached in the *cis* position relative to the bridge, then the shift at Ru_a compared to Ru_b drops and now we find $m = 0.49$. It is important to note that the m values listed in Tables III and V represent the experimental ratio $(\delta E_{1/2}(Ru_a))/(\delta E_{1/2}Ru_b))$, which corresponds to the synthetic transformation of replacing one of the ammine ligands at one end of the symmetric decaammine dimer with some unique ligand L (see Figures 1–4)

$$[\text{symmetric}]\ (NH_3)_5Ru\text{–}L_{br}\text{–}Ru(NH_3)_5^{4+} \rightarrow$$

$$[\text{asymmetric}]\ cis/trans\text{-}L(NH_3)_4Ru_a\text{–}L_{br}\text{–}Ru_b(NH_3)_5^{4+}$$

The average m value over the *trans*-substituted, pz-bridged series is 0.90 ± 0.27; for the *cis*-substituted dimers it is 0.59.

A major trend which emerges from the data in Table III is that as the redox perturbation is increased, the observed bandwidth at half-height, $\Delta\nu_{1/2}$, of the IT band rapidly increases. For example the relatively narrow and characteristically Robin and Day class III (valence delocalized)[2,38] value of 0.184 eV for the Creutz–Taube ion widens to 0.510 for L = bpy (entry number 7)—a value corresponding to the class II (valence localized) category of Robin and Day. For the asymmetric *trans*-py dimer we observe $\Delta\nu_{1/2}$ = 0.300 eV—an intermediate case.

In the *trans*-L, asymmetric 4CP-bridged series (Table V) we see much smaller m values (average = 0.14 ± 0.03) and only a very slight possible trend in the $\Delta\nu_{1/2}$ values.

(38) Robin, M. B.; Day, P. *Adv. Inorg. Chem. Radiochem.* **1967**, *10*, 247–403.

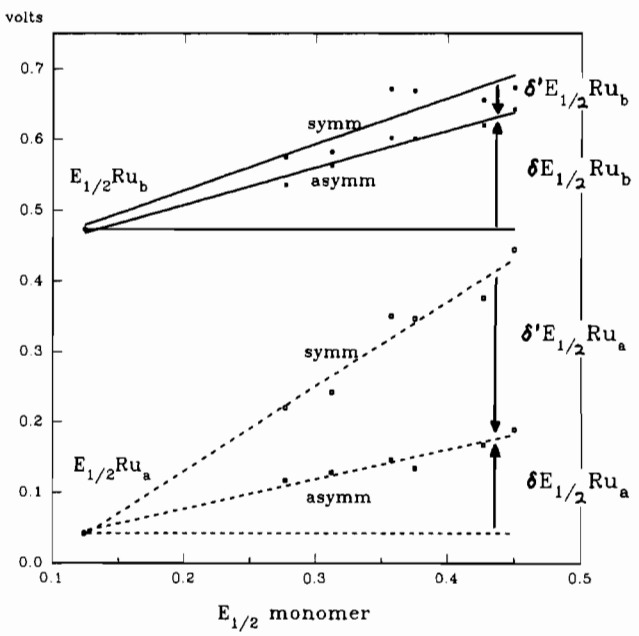

Figure 4. Schematic illustration of how the quantities m and m' can be calculated using the slope ratios from Figures 2 and 3. $m \cong (\delta E_{1/2}(Ru_a))/(\delta E_{1/2}(Ru_b))$ for the asymmetrical dimers, and $m' \cong (\delta' E_{1/2}(Ru_b))/(\delta' E_{1/2}(Ru_a))$ for the symmetric series.

The electrochemical and spectroscopic data for the corresponding *symmetrically* substituted dimers, $(LA_4Ru)_2L_{br}^{4+/5+/6+}$ are summarized in Tables IV an VI. For the pyrazine-bridged series (Table IV), we note that one major difference from the asymmetric dimers is that now $\Delta E_{1/2}$ *decreases* as we proceed down the table to stronger π-back-bonding ligands. The same is also true to a lesser extent for the 4CP-bridged series (Table VI). For the pz-bridged series we see that even though $\Delta E_{1/2}$ is decreasing, $\Delta\nu_{1/2}$ steadily increases down the series—an important point to which we will return.

In Tables IV and VI for the symmetrical dimers we list the

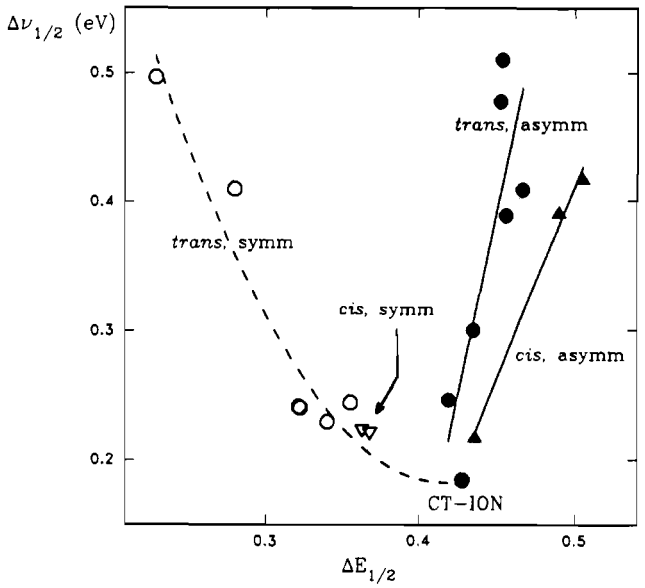

Figure 5. Observed behaviors of the IT bandwidth, $\Delta\nu_{1/2}$, and the potential difference $\Delta E_{1/2}$ between the first and second metal oxidations for the pz-bridged series of dimers (data from Tables III and IV).

experimental ratio m', which is defined as $\delta' E_{1/2}(Ru_b))/\delta' E_{1/2}(Ru_a))$ for the synthetic transformation

$$[\text{asymmetric}]\ cis/trans\text{-}LA_4Ru_b\text{–}L_{br}Ru_aA_5 \rightarrow [\text{symmetric}]\ (cis/trans\text{-}LA_4Ru)_2L_{br}$$

Significantly, the m' values for the symmetrical dimers are found to be considerably smaller than the m values listed in Tables III and V. The importance of this point will be discussed in a later section. For the pz-bridged *trans*-series we find $m'(\text{av}) = 0.25 \pm 0.11$ and for the *cis*-series we find $m'(\text{av}) = 0.32$. The difference between the two values is probably insignificant given the scatter in the data. For the *trans*-substituted 4CP series (Table VI), we find $m'(\text{av}) = 0.052 \pm 0.025$.

An alternative way in which to characterize the shift ratios m and m' is consider the slopes of plots of $E_{1/2}(Ru_a)$ and $E_{1/2}(Ru_b)$ for the various dimers as progressively stronger perturbation is applied relative to the decammine species. If we use the monomer potential, $E_{1/2}(LA_4RuL_{br}^{2+/3+})$, as a measure of the strength of the applied perturbation, then we can generate Figures 2 and 3. The behaviors of the two asymmetric dimer series are as shown in Figures 2a and 3a. The overall effective shift ratio for the pz- and 4CP-bridged dimers is then just equal to the ratios of the slopes of the best-fit lines for $E_{1/2}(Ru_a)$ and $E_{1/2}(Ru_b)$. For pz we find $m \cong 0.418/0.523 = 0.80$. For 4-CP as bridge we find $m \cong 0.117/0.831 = 0.14$. The data for the symmetric dimers are displayed in Figures 2b and 3b. For these series, the m' ratios are equal to the *differences* of the slopes between the symmetric and asymmetric series. This relationship is illustrated graphically in Figure 4. Over the pz-bridged series we obtain $m' \cong (0.652 - 0.523)/(1.202 - 0.418) = 0.17$. This value is in reasonable agreement with the value of 0.25 ± 0.11 arrived at above. For 4-CP we find $m' \cong (0.879 - 0.831)/(1.123 - 0.117) = 0.05$—essentially exact agreement with the previous value.

Bandwidth Effects in the Pyrazine-Bridged Series. Examining the data in Tables III and IV shows that one of the more interesting relationships between measureable properties for these dimers (asymmetric and symmetric pz-bridged, respectively) is the one which exists between the differential pulse polarographic peak splitting, $\Delta E_{1/2}$, and the intervalence transfer (IT) absorption bandwidth at half-height, $\Delta\nu_{1/2}$. Figure 5 illustrates this relationship graphically. It is clear that the redox asymmetry induced by substitution of increasingly dπ-electron density withdrawing ligands on *one* side of the asymmetric dimers leads to a much more rapid widening of the IT band, and by inference a delocalized → localized change in electronic structure, than does the addition of dπ-electron withdrawing ligands to *both* sides as in the symmetric series. Additionally, it would appear that redox asymmetry induced by *trans* substitution (filled circles) is somewhat more effective than *cis* substitution (filled triangles) in bringing about the delocalized → localized change in electronic structure.

In the symmetric series, the rate of widening in $\Delta\nu_{1/2}$ which attends the increasing demand on the dπ-electron density at the metal ions by the terminal ligands L does not appear to be much affected by the position of the substitution (note the open circles and triangles on same trendline in Figure 5). The decrease in $\Delta E_{1/2}$ as dπ-electron density is withdrawn from the dimer was not properly taken account of in our early work on these systems.[6] The significance of this will be discussed in a later section.

Rhodium Analogues $L(NH_3)_4Ru^{II/III}L_{br}Rh^{III}(NH_3)_5^{5+/6+}$ of the Asymmetric Series. In Tables IV and VI for the symmetric pz- and 4CP-bridged series, respectively, we list electrochemical potential data obtained for several rhodium analogues of the formula shown above. These molecules were examined with the idea that the degree of valence delocalization in a given diruthenium dimer might be reflected in the electrochemical potential difference between the $E_{1/2}(Ru_b)$ peak in the diruthenium case and the single $Ru^{II/III}$ couple of the rhodium–ruthenium dimer (the $Rh^{III}(NH_3)_5^{3+}$ fragment is electrochemically inactive over the potential range of the dimers). Any special thermodynamic stabilization of the mixed-valence (dπ^6,dπ^5) diruthenium dimer arising from electronic delocalization would be absent in the electrostatically identical but fully dπ-saturated (dπ^6,dπ^6) $Ru^{II}Rh^{III}$ dimer. This strategy was used by Creutz and Taube in their pioneering investigations[3] of mixed-valence binuclear complexes and subsequently by Moore *et al.* in an extensive investigation of binuclear complex photochemistry.[39] It has also been critically discussed by Richardson and Taube in a review of this area.[14b]

Creutz and Taube obtained a shift in the $Ru^{II/III}$ redox potential of –0.050 V for the synthetic transformation of replacing a ruthenium(III) pentaammine moiety with a rhodium one,

$$(NH_3)_5Ru^{II/III}pzRu^{III}(NH_3)_5^{5+/6+} \rightarrow (NH_3)_5Ru^{II/III}pzRh^{III}(NH_3)_5^{5+/6+}$$

(potential measured at pH 1 in 0.1 M KCl). Moore *et al.* obtained a value of –0.057 V in neutral 0.1 M KCl.[39] Our value listed in Table III is –0.067 V (measured in 0.1 M TEA(PF_6)/acetonitrile). Including the three *trans*-substituted, pz-bridged dimers listed in Table III, we find an average value of 0.056 V. For 4CP as bridge, we find –0.025 V for the decaammine species and an average of –0.014 V over the series (Table V). This is in qualitative agreement with the expectation of a decreased coupling between metals in the 4CP-bridged case relative to pz, but it is somewhat smaller than what might be expected given the value of –0.019 V found by Moore *et al.* for the longer 4,4′-bpy-bridged decaammine.[39] We note, however, that the error limits for these quantities are on the order of ±0.008 V; hence, all that can rigorously concluded is that the two appear to be comparable within error. Implications of the potential data for the rhodium analogues with regards to resonance stabilization in these complexes will be discussed in a later section.

Mulliken Formalism and Electronic Coupling. In this section we will briefly describe some of the aspects of the Mulliken treatment of donor–acceptor interactions and show how the approach can be used in conjunction with electrochemical potential data in such a way as to address the issue of electronic coupling in mixed-valence dimeric systems.

(39) Moore, K. J.; Lee, L.; Mabbott, G. A.; Petersen, J. D. *Inorg. Chem.* **1983**, *22*, 1108–1112.

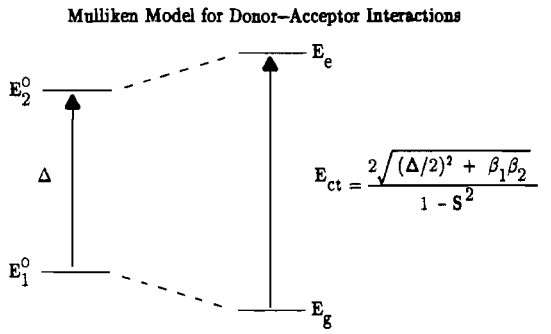

Figure 6. Simple two-state mixing scheme used in Mulliken's theoretical analysis of donor–acceptor interactions.[8]

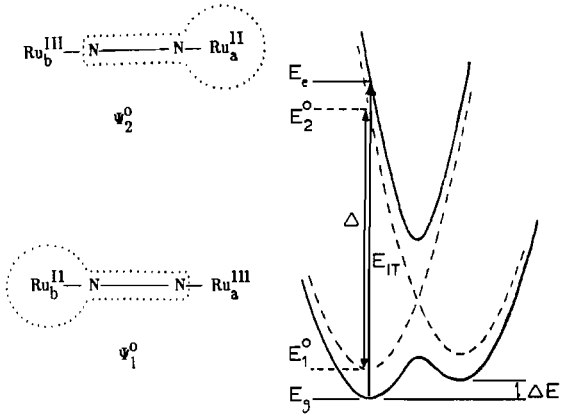

Figure 7. Application of the Mulliken model to the mixed-valence dimer case.

Figure 6 illustrates the mixing scheme used by Mulliken in the development of his simplified resonance structure theory of charge-transfer complexes.[8,9] The basis set consists of the hypothetical zero-order "no bond" state $\Psi_1^0(D,A)$, which has the exchanging electron fully localized on the donor site, and the "dative" state $\Psi_2^0(D^+,A^-)$, where the electron is fully localized on the acceptor site. These two starting wave functions are mixed using a variational treatment so as to give rise to stabilized ground-state wave function Ψ_g and a destabilized, excited-state combination, Ψ_e. The forms of the resulting wave functions are written as

$$\Psi_g = a\Psi_1^0(D,A) + b\Psi_2^0(D^+,A^-) \qquad \Psi_e = a^*\Psi_2^0(D^+,A^-) - b^*\Psi_1^0(D,A) \quad (5)$$

The energies E_g and E_e are found to be

$$E_{e,g} = \frac{1}{(1-S^2)}\left[\frac{E_1^0 + E_2^0}{2} - \mathbf{SH} \pm ((\Delta/2)^2 + \beta_1\beta_2)^{1/2}\right] \quad (6)$$

where the following definitions apply

$$\mathbf{S} = \langle\Psi_1^0|\Psi_2^0\rangle \qquad \mathbf{H} = \langle\Psi_1^0|\hat{H}|\Psi_2^0\rangle$$

$$\beta_i = \mathbf{H} - \mathbf{S}E_i^0 \qquad \Delta = E_2^0 - E_1^0$$

The quantity E_1^0 pertaining to the no-bond basis wave function is taken as the energy of donor's HOMO relative to vacuum and is generally equated with the ventrical ionization potential of the isolated donor with small corrections to reflect the proximity of the acceptor.[40] Figure 7 shows how the Mulliken formalism applies to the case of mixed-valence binuclear complexes such as the ones used in this study. A major point of difference compared to the organic donor–acceptor complexes typically addressed using this theory is that now most (or all if $\Delta E = 0$) of the zero-order splitting Δ originates in the Franck–Condon energy associated with the vertical electron transfer.

Of central interest to us are the wave function coefficients a and b of eq 5. Mulliken derived the following expressions for their ratio:

$$\rho \equiv b/a = -\frac{(E_1^0 - E_g)}{(\mathbf{H} - \mathbf{S}E_g)} = -\frac{(\mathbf{H} - \mathbf{S}E_g)}{(E_2^0 - E_g)} \quad (7)$$

Rearranging these expressions leads to (8) and (9),

$$\rho(\mathbf{H} - \mathbf{S}E_g) = E_g - E_1^0 \quad (8)$$

$$\rho(E_g - E_2^0) = \mathbf{H} - \mathbf{S}E_g \quad (9)$$

Solving (8) and (9) for either **H** or **S** and equating the resulting expressions leads to (10),

$$\rho = \left(\frac{E_g - E_1^0}{E_g - E_2^0}\right)^{1/2} \quad (10)$$

Our approach to finding a link between electrochemical potential shift data and the quantity ρ rests upon the idea that by perturbing one end of a mixed-valence dimer through ligand substitution we can, in effect, vary the energy E_1^0 independently of E_2^0 or *vice versa*. If we can then obtain information about how E_g and E_e respond to this perturbation because of their quantum coupling to E_i^0, we can assess the ratio ρ.

Making reference to Figure 8, it can be seen that a perturbation δE_1^0 in the energy of the no-bond state will give rise to perturbations δE_g^f and δE_g^d in the favored and disfavored redox isomers of the ground state of the system (the superscripts f and d signify that we are referring to the *favored* and *disfavored* redox isomer in the case of the right-hand surfaces where there is now a redox asymmetry). There will also be a downward shift δE_e^f in the energy of the excited-state of the favored redox isomer with a magnitude very nearly equal to δE_g^d. An important underlying assumption here is that the surfaces are harmonic and that the ligand substitution process does not significantly change their shapes or displacement in nuclear configurational space. The new redox asymmetry of the dimer, ΔE, will effect the electrochemical potential difference between the first and second oxidations of the dimer, $\Delta E_{1/2}$, in a predictable way.

From Figure 8, we see that the most directly relevant quantities we might try to calculate from theory would then be $\delta E_g/\delta E_1^0$ and $\delta E_g^d/\delta E_1^0$. Changing from finite increments to partial differentials and making reference to eq 6, we find equations (11) and (12),

$$\partial E_g^f/\partial E_1^0 = \frac{1}{\sigma}\left[1/2 - \mathbf{S}(\partial\mathbf{H}/\partial E_1^0) - \frac{1}{2R}(-\Delta/2 + (\beta_1 + \beta_2)(\partial\mathbf{H}/\partial E_1^0) - \mathbf{S}\beta_2)\right] \quad (11)$$

$$\partial E_g^d/\partial E_1^0 = \frac{1}{\sigma}\left[1/2 - \mathbf{S}(\partial\mathbf{H}^d/\partial E_1^0) - \left(\frac{1}{2R^d}\right)(\Delta^d/2 + (\beta_1^d + \beta_2^d)(\partial\mathbf{H}^d/\partial E_1^0) - \mathbf{S}\beta_1^d)\right] \quad (12)$$

where $\sigma = 1 - S^2$ and the other variables are as defined previously.[41]

The readily measurable experimental quantity we wish to relate to the quantum coupling in the system is the electrochemical potential shift ratio $m = (\delta E_{1/2}(Ru_a))/(\delta E_{1/2}(Ru_b))$, which obtains upon ligand substitution. The theoretical quantity of relevance

(40) See ref 8b, Chapter 9.

(41) In deriving (11) and (12), we have used the relations $\partial E_1^{0d}/\partial E_1^0 = 0$, $\partial E_2^{0d}/E_1^0 = 1$, and $\Delta^d = E_2^{0d} - E_1^{0d}$, where the superscript d indicates that these quantities correspond to the *disfavored* redox isomer in Figure 8 (the higher-lying curve of the pair on the right-hand side of the figure).

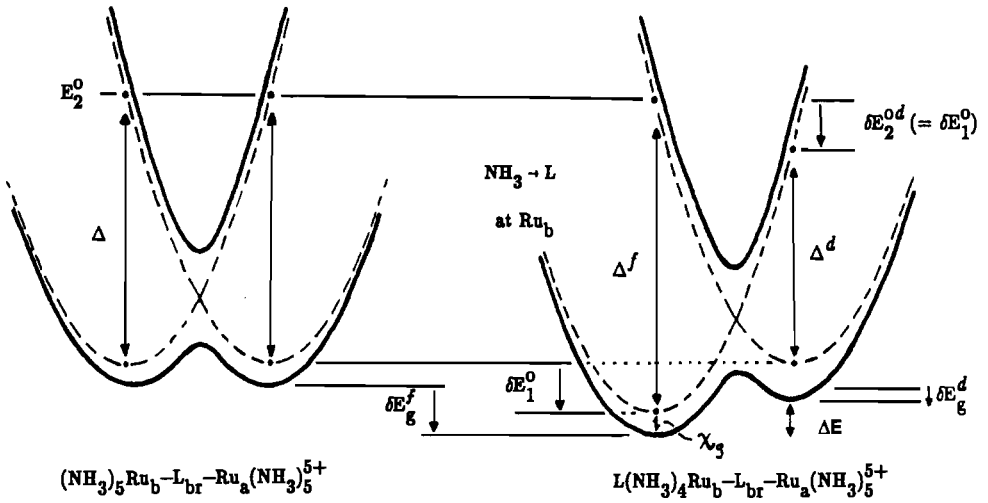

Figure 8. Schematic illustration of how the potential surfaces respond to ligand substitution processes.

is clearly the ratio which we will denote by n:

$$n \equiv (\partial E_g^d/\partial E_1^o)/(\partial E_g^f/\partial E_1^o) \quad (13)$$

The nature of the relationship between the experimental ratio m and the theoretical quantity n will be discussed in detail in a later section. Substituting eqs 11 and 12 into eq 13 yields a theoretical expression for n. In the limit that $\partial \mathbf{H}/\partial E_1^o \cong 0$ and $\delta E_1^o \ll \Delta$, such that $\Delta^f \cong \Delta^d$, $\beta_i^f \cong \beta_i^d$, and $R^f \cong R^d$, we find

$$n = \frac{R - \Delta/2 + \mathbf{S}\beta_1}{R + \Delta/2 + \mathbf{S}\beta_2} \quad (14)$$

where R is the square root term in eq 6, $((\Delta/2)^2 + \beta_1\beta_2)^{1/2}$. Solving for R in eq 14 yields

$$R = \frac{1}{(n-1)}[-(\Delta/2)(n+1) + \mathbf{S}\beta_1(1-n) + n\mathbf{S}^2\Delta] \quad (15)$$

where we have used the identity $\beta_2 = \beta_1 - \mathbf{S}\Delta$.

Combining eqs 6 and 10, we can readily write an expression for ρ,

$$\rho = \left[\frac{(E_1^o + E_2^o)/2 - \mathbf{SH} - R - E_1^o\sigma}{(E_1^o + E_2^o)/2 - \mathbf{SH} - R - E_2^o\sigma}\right]^{1/2} = \left[\frac{\Delta - 2(S\beta_1 + R)}{-\Delta - 2(S(\beta_1 - S\Delta) + R)}\right]^{1/2} \quad (16)$$

In the limit of small S, this expression reduces to the remarkably simple result

$$\rho = \sqrt{n} \quad (17)$$

The same logic and mathematics can be applied to the alternative experimental shift ratio $m' = (\delta E_{1/2}(Ru_b))/(\delta E_{1/2}(Ru_a))$ obtained when we directly perturb E_2^o by replacing ligand L with NH_3 at Ru_a in $L(NH_3)_4Ru_b-L_{br}-Ru_a(NH_3)_4L$.[42] Now the theoretical quantity of interest is $n' \equiv (\partial E_g^f/\partial E_2^o)/(\partial E_g^d/\partial E_2^o)$, and we again obtain eqs 16 and 17 but with n' replacing n.

Relationship between the Electrochemical Potential Shift Ratios m and m' and the Electronic Coupling. The redox asymmetry in a given dimeric system, as depicted by the quantity ΔE in Figure 8, contributes directly to the observed differential pulse polarographic peak splitting $\Delta E_{1/2}$ illustrated in Figure 1. ΔE is not the only source of the peak splitting, however, and the various contributions to $\Delta E_{1/2}$ have been discussed by Sutton *et al.*[37] and by others.[14b,39,43-46] For complexes of the kind studied in this work, there will be five primary contributions to $\Delta E_{1/2}$,

$$\Delta E_{1/2} = \Delta E_{deloc} + \Delta E_{coul} + \Delta E_{stat} + \Delta E_{induct} + \Delta E \quad (18)$$

ΔE_{deloc} represents the splitting due to resonance stabilization of the mixed-valence state relative to either to 2,2 or 3,3 isovalent states. This splitting will have the effect of increasing $E_{1/2}(Ru_b)$ and decreasing $E_{1/2}(Ru_a)$ by an amount equivalent to magnitude of χ_s—the resonance stabilization depicted in Figures 6 and 7. It is generally thought to be a quite minor contribution. We would point out, however, that part of the reason for concluding this has been based on the use of eq 4 for assessing the magnitude of the resonance interaction. The ΔE_{coul} term represents the decreased electrostatic repulsion in the 2,3 oxidation state relative to the 2,2 and 3,3 parent states. ΔE_{stat} is the "statistical" contribution to the stability of the 2,3 state in symmetric $\Delta E = 0$ systems relative to the parent states. ΔE_{induct} is a term that has to do with the inductive and π-back-bonding effects that specifically destabilize the 2,2 state relative to the 2,3 state in systems such as the ones used in this study.[37]

The ΔE_{stat} term is at a maximum of 36 mV for $\Delta E = 0$ and will fall off toward 0 as ΔE (true redox asymmetry) about surpasses 60 mV.[45] The ΔE_{coul} term will be primarily a function of the distance between the charge centers and the dielectric constants of the intervening medium and the solvent medium surrounding the dimer.[37b,44,47] Sutton *et al.*, have shown that this term makes a small but significant contribution to the peak splitting in fairly weakly coupled systems such as the 4,4'-bipyridine-bridged decaammine dimer.[37] Its contribution would be expected to increase in the dimers studied in this work due to the shorter bridge lengths. Since the metal–metal distance is constant over each of the series which we use in our comparisons, however, we will assume that the ΔE_{coul} term remains constant as well.

The largest contribution to the peak splitting according to the work of Sutton *et al.* is the ΔE_{induct} term. This term arises from a combination of two effects. The first is due to the decreased

(42) The situation is now similar to that depicted in Figure 8 except that the product's potential surface moves *up* in energy upon synthetic manipulation. In this case, we make note of the relations $\partial E_1^{od}/\partial E_2^o = 1$ and $\partial E_2^{od}/\partial E_2^o = 0$.

(43) Gange, R. R.; Spiro, C. L.; Smith, T. J.; Hamann, C. A.; Thies, W. R.; Shiemke, A. K. *J. Am. Chem. Soc.* **1981**, *103*, 4073–4081.
(44) Palaniappan, V.; Singru, R. M.; Agarwala, U. C. *Inorg. Chem.* **1988**, *27*, 181–187.
(45) Dose, E. V. *Inorg. Chim. Acta* **1981**, *54*, L125–L127.
(46) Ernst, S.; Kasack, V.; Kaim, W. *Inorg. Chem.* **1988**, *27*, 1146–1148.
(47) (a) Ehrenson, S. *J. Am. Chem. Soc.* **1976**, *98*, 7510–7514. (b) Brunschwig, B.; Ehrenson, S.; Sutin, N. *J. Phys. Chem.* **1986**, *90*, 3657–3668.

π-acid nature of the bridging ligand in a 2,2 dimer relative to a 2,3 dimer. We might describe this effect as "π^* overcrowding" at the bridging ligand. The first oxidation of the complex to form the 2,3 dimer is thus made anomalously easy compared to either the second oxidation or, in most cases, to the appropriate monomeric compound. The magnitude of the destabilization of the II,II oxidation state is made clear by comparing the redox potential data in Tables I, III, and IV where we see that the +2/+3 oxidations of the (+2) charged monomers are actually at higher potentials than the first (Ru_a; +4/+5) symmetric dimer oxidations in spite of the significantly higher charges on the dimers. The second aspect arises as result of the inductive effect of the coordinated Ru_a^{III} ion on the bridging ligand π^* levels in the mixed-valence dimer. The $A_5Ru_a^{III}L_{br}Ru_b^{II/III}A_4L^{5+/6+}$ potential is thus increased relative to the $LA_4RuL_{br}^{2+/3+}$ monomer couple due to the greater π-acidity of the bridging unit toward Ru_b^{II}.

As shown in Figure 8, replacing an ammine ligand on a decaammine dimer with a substituted pyridine ligand L will clearly increase (create) the redox asymmetry ΔE by pulling down E_1°. This will show up as an increase in the observed electrochemical peak splitting. Importantly, however, this same synthetic operation also has the potential to change the magnitudes of the ΔE_{deloc}, ΔE_{stat}, and ΔE_{induct} terms. Specifically, ΔE_{deloc} will decrease due to the increased value of Δ (see Figures 6 and 7) and the resulting attenuation of the resonance interaction (note eq 6). ΔE_{induct} will decrease due to the decreased dπ-electron density on Ru_b (there will now be competition for the dπ electron density at Ru_b between the bridging ligand and new ligand L). Additionally, the ΔE_{stat} contribution will fall off from its maximum value of 36 mV.

The consequence of the changes in ΔE_{deloc}, ΔE_{stat}, and ΔE_{induct} with substitution at Ru_b is that the shift ratio $m = (\delta E_{1/2}(Ru_a))/(\delta E_{1/2}(Ru_b))$ will be made larger than what would be expected if indeed $m \cong n = (\delta E_g^d/\partial E_1^\circ)/(\partial E_g^f/\partial E_1^\circ)$. The reason for this is that the downward changes in ΔE_{deloc}, ΔE_{stat}, and ΔE_{induct} cause $\delta E_{1/2}(Ru_a)$ to be a larger positive number than it would be otherwise. Thus the coupling between the bond and no-bond basis states that would be deduced using the measured m value and eq 16 or 17 would be an overestimate. For this reason, it is also necessary to consider the complementary experimental ratio m' and the synthetic operation in which L is replaced by ammine at Ru_a on a symmetric, disubstituted dimer,

$$L(NH_3)_4Ru_b\text{–}L_{br}\text{–}Ru_a(NH_3)_4L^{4+} \rightarrow L(NH_3)_4Ru_b\text{–}L_{br}\text{–}Ru_a(NH_3)_5^{4+}$$

Now the situation is such that the ΔE_{deloc} term will decrease due to the increased value of Δ in the resulting asymmetric dimer. In principle, the magnitude of this contraction in $\Delta E_{1/2}$ should be somewhat less than in the previously discussed synthetic transformation since the spectroscopic data indicate that delocalization is attenuated in the symmetric $(LA_4Ru)_2L_{br}$ dimers relative to the (symmetric) decaammine dimers (note the left-hand curve in Figure 5[48]). Once again, the ΔE_{stat} term will fall off from 36 mV. Both of these changes act to depress $\Delta E_{1/2}$ in the asymmetric dimers relative to the symmetric, disubstituted ones; thus they will act to make m' too large since both cause $\delta' E_{1/2}(Ru_a)$ to decrease in magnitude. Similarly, the magnitude of $\delta' E_{1/2}(Ru_b)$ is increased by the dropping away of the ΔE_{stat} contribution. The change in ΔE_{deloc} does *not* introduce an artifact into $\delta' E_{1/2}(Ru_b)$ since $E_{1/2}(Ru_b)$ and E_g of the Mulliken model are directly related in our treatment. Importantly, the change in the ΔE_{induct} term and its impact on $\delta E_{1/2}(Ru_a)$ is now in the *opposite* direction than in the previous synthetic transformation. This can be understood if we consider ligand additivity effects.[49] The inductive destabilization of the 2,2 oxidation state (and the resulting cathodic shift in the Ru_a reduction potential) arising from "π^* overcrowding" at the bridge will be less in the symmetrically disubstituted dimers than in either the asymmetric monosubstituted analogues or the decaammine species due to the fact that the relative impact of the π-acid strength of the bridging ligand L_{br} will be attenuated by the presence of L on Ru_a and the resulting competition for dπ electron density at Ru_a. The increase in ΔE_{induct} upon going from the symmetric disubstituted to the asymmetric monosubstituted configuration will manifest entirely in the magnitude of $\delta E_{1/2}(Ru_a)$ and will have the effect of making $\delta E_{1/2}(Ru_a)$ a larger negative number than it would be otherwise (the inductive effect of the Ru_a^{III} unit coordinated to the bridge on the value of $E_{1/2}(Ru_b)$ will not depend on whether Ru_a is in a pentaammine or a tetraammine L coordination environment). Thus $m' = (\delta' E_{1/2}(Ru_b))/(\delta' E_{1/2}(Ru_a))$ will be diminished.

We have no direct way to separate and compare the opposing influences of the changes in ΔE_{deloc}, ΔE_{stat}, and ΔE_{induct} on m'. Estimates of the resonance stabilization χ_g based on potential data from the rhodium analogues taken in conjunction with the potential data on the symmetric dimers, however, do indicate that ΔE_{induct} is probably the larger effect. The χ_g stabilization energies for the various symmetrical dimers for which rhodium analogues were studied are listed in Table VII. These values are arrived at by comparing the observed value for the potential of the $A_5Rh^{III}L_{br}Ru^{II/III}A_4L^{5+/6+}$ couple with the $E_{1/2}(Ru_b)$ value for the corresponding symmetrical dimer (corrected for ΔE in the case of the pz-bridged dimers). Inspecting the values for the two series, we see that there is no obvious drop-off in the resonance stabilization as the terminal ligands become more electron-withdrawing. This rather surprising result is counter to our expectations and to trends in delocalization based on intervalence-transfer absorption data (vide infra). At the same time, we note that the slopes of the $E_{1/2}(Ru_a)$ vs $E_{monomer}$ plots in Figures 2 and 3 both considerably exceed unity. The apparent lack of variation in χ_g (and hence ΔE_{deloc}) over the range of monomer potentials used here combined with the observation of these large slopes for $\Delta E_{1/2}(Ru_a)$ indicate that the primary additional effect operating on $E_{1/2}(Ru_a)$ over the symmetric series is in fact the one due to variations in ΔE_{induct} as L is varied. This would imply that m' is likely to be decreased by the upward change in ΔE_{induct} more than it is increased by the changes in ΔE_{deloc} and ΔE_{stat} when L is taken to ammine at Ru_a.

Table VII. Thermodynamic Resonance Stabilization Energies χ_g As Determined by Comparing the Redox Potentials of Selected Diruthenium and Heterobimetallic Ruthenium/Rhodium Dimers

L	*trans*-$(LRu(NH_3)_4)_2L_{br}^{5+/6+}$, $E_{1/2}(Ru_b)$	*trans*-$L(NH_3)_4RuL_{br}Rh(NH_3)_5^{5+/6+}$, $E_{1/2}(Ru)$	χ_g
	L_{br} = pz		
(1) NH_3	0.473[a]	0.392	–0.063[b]
(2) py	0.582	0.533	–0.031
(3) 3-Clpy	0.672	0.564	–0.090
(4) 3-Fpy	0.669	0.512	–0.139
	L_{br} = 4CP		
(1) NH_3	0.331	0.306	–0.025
(2) py	0.475	0.462	–0.013
(3) 3-Clpy	0.525	0.504	–0.021
(4) 4-Brpy	0.515	0.492	–0.023

[a] All potentials in volts *vs* ferrocene/ferrocenium. [b] In the case of pz as bridge, the χ_g value is corrected for the 18-mV anodic shift expected in $E_{1/2}(Ru_b)$ due to ΔE_{stat} in the symmetrical dimers (see text). Note: This contribution of $\Delta E_{1/2}$ is not present in the 4CP case due to the asymmetry of the bridge itself.

(48) The progressive widening of the IT band in the symmetrical pz-bridged series as stronger and stronger perturbation is applied would be consistent with the generally accepted idea that IT bands are characteristically narrow in valence-delocalized dimers and characteristicially wider in localized systems with bandwidths predicted by the equation due to Hush, $\Delta\nu_{1/2} = (2310(E_{op} - \Delta E))^{1/2}$ [1a,2]

(49) Bursten, B.; Green, M. R. *Prog. Inorg. Chem.* **1988**, *36*, 393–485.

From all of the foregoing, we conclude that the electronic coupling computed on the basis of the experimental ratio m will be too high. The coupling based on the m' ratio will most likely be too low, but we cannot confidently assess by how much. We will take the coupling calculated on the basis of m' as a reasonable lower limit to the true value.

Mines *et al.* have applied the electrochemical potential shift ratio approach described here to the problem of assessing the degree of electronic coupling between the metal and π-back-bonding ligand in mononuclear complexes such as $Ru(NH_3)_4(phen)^{2+}$.[19] Here the situation is simpler and the interpretation of the shift ratio is more straightforward. Because there is no central π-back-bonding bridging unit mediating the interaction between the redox sites, there is no special inductive destabilization of the fully reduced form of the system—in this case $Ru^{II}(NH_3)_4(phen^{-})^{+}$. Since there is no possibility for electron delocalization from the reduced phen π^* level into the filled $d\pi$ levels of the Ru(II), then variations in the energies of the $d\pi$ levels through, for example, solvent donicity changes cannot directly effect the energy of an electron in the HOMO of the fully reduced complex (a phen π^* level in this case). For this reason, shifts in the $Ru^{II}(NH_3)_4(phen)^{2+/1+}$ couple as the metal $d\pi$ levels are manipulated (or *vice versa*) can be simply related to the coupling between the $d\pi$ levels and the empty phen π^* LUMO in the 2+ complex.

Two subtleties in the data bear mentioning at this point. From Table III we see that for the asymmetric pz-bridged series the shift ratio m appears to decrease somewhat with stronger redox perturbation down the series. This might be expected if either of the contributions to m from changes in ΔE_{deloc} or ΔE_{induct} reaches a natural limit as we progress down the series or if the change in electronic structure from delocalized to localized (as evidenced by the IT bandwidth variations) shows up in the observed m. Second, the observation that m drops for *cis*-substituted relative to *trans*-substituted asymmetric dimers is in keeping with the idea that competition for $d\pi$ electron density is important since in the *cis* case competition will be attenuated due to the orthogonality of the metal orbitals involved.

Application of the Mulliken Formalism. Equations 6–17 provide us with the means to analyze our mixed-valence dimeric systems and assess the degree of electronic coupling within the context of the Mulliken model. Prior to beginning this analysis, however, it is useful to consider the probable magnitude of the overlap integral $S = \langle \Psi_1^o | \Psi_2^o \rangle$ relevant to each of our two bridging ligands, pyrazine and 4-cyanopyridine. Creutz has developed and applied a straightforward molecular orbital scheme for estimating the ligand π^* contribution to the highest occupied molecular orbital for ruthenium pentaammine and tetraammine complexes of nitrogen heterocyclic ligands.[50] In their recent application of this approach to the Creutz–Taube ion they calculate possible values of 0.37 and 0.51 for the coefficient of the pyrazine π^* orbital in the HOMO of the ion (depending on the details of the model chosen). If we take the middle of this range, 0.44, as a reasonable estimate, then this would imply an S value of on the order of $(0.44)^2 \cong 0.2$ for the overlap of Ψ_1^o and Ψ_2^o in our application of Mulliken theory to the pyrazine-bridged series of dimers.

This estimate is based purely on an "electron-transfer" coupling pathway, as is the depiction of the coupling between Ψ_1^o and Ψ_2^o given in Figure 7. Hupp[51] as well as Richardson and Taube[14a] have both pointed out that substantial coupling can occur through a "hole-transfer" pathway involving superexchange between the metal sites via higher-lying ligand-to-metal charge-transfer states. Participation of this pathway would presumably give rise to a second, additive contribution to the total effective overlap.[52]

For the 4-cyanopyridine bridge, we make reference to the data and molecular orbital approach used by Richardson and Taube in the course of their work on electronic coupling in mixed-valence dimers. From their data on the pentaammineruthenium(4CP)$^{2+}$ monomer, we calculate a ligand π^* coefficient of 0.38; thus, our estimate for S becomes $(0.38)^2 \cong 0.14$ for the 4CP-bridged series.

From eq 6 it follows that the charge-transfer energy can be written as

$$E_{op} = 2R/(1 - S^2) \tag{19}$$

where $R \equiv [(\Delta/2)^2 + \beta_1(\beta_1 - S\Delta)]^{1/2}$. If we correct the observed IT band energy for the contribution arising from spin–orbit coupling effects,[53,54] then eq 19 allows us to estimate a value of R from E_{op} at any given S. Equation 15 for R as a function of n, S, β_1, and Δ can be solved for Δ to yield

$$\Delta = [(n-1)(R - S\beta_1)]/(S^2 n - (1+n)/2) \tag{20}$$

Using R calculated from E_{op} and S, n as approximated from the electrochemical shift ratio m', and an initial guess for β_1 (a negative number), we can then calculate a value for Δ.

Using the expanded form of R in eq 19, the following expression for β_1 can be solved:

$$\beta_1 = [S\Delta - (S^2\Delta^2 - (\Delta^2 - E_{op}^2(1 - S^2))^{1/2}]/2 \tag{21}$$

Iteration between (20) and (21) leads to a consistent pair of Δ and β values for given values of E_{op}, S, and m'. The wave function coefficient ratio ρ can then be calculated using eq 16. The results of such calculations on the symmetrical pz and 4CP-bridged dimers are shown in the first four columns of Tables VIII and IX. The average values of β_1, Δ, and ρ obtained at S = 0.2 for the pz-bridged series are –0.19 eV, 0.27 eV, and 0.51, respectively. For the 4CP series at S = 0.14 we find the following average values: β_1 = –0.22 eV, Δ = 0.82 eV, and ρ = 0.24.

Having consistent values for β_1 and Δ, we are now able to calculate an estimate for the predicted resonance stabilization of the ground state due to electron delocalization. The resonance stabilization is described by Mulliken as[8]

$$\chi_g = E_g - E_1^o \tag{22}$$

where E_g, E_1^o, and χ_g are as illustrated in Figure 6. Using perturbation theory Mulliken derived the following approximate formula for χ_g in the limit that $(\Delta/2)^2 \gg \beta_1\beta_2$:

$$\chi_g \cong -(\beta_1)^2/\Delta \tag{23}$$

In the 4CP case, the limiting condition is approximately satisfied since $(\Delta_{av}/2)^2 = 0.166$ and $\beta_1\beta_2 = \beta_1(\beta_1 - S\Delta) = 0.071$. Equation 23 then predicts χ_g = –0.057 eV.

For the pz-bridged series, the limiting condition is clearly not met; $(\Delta_{av}/2)^2 = 0.018$ and $\beta_1\beta_2 = 0.047$. A more exact expression for χ_g can be obtained by using eq 6 for E_g in eq 22,

$$\chi_g = [\Delta - 2S\beta_1 - (\Delta^2 + 4\beta_1^2 - 4S\beta_1\Delta)^{1/2}]/(2(1 - S^2)) \tag{24}$$

The predicted value of χ_g for the pz-bridged series is then calculated to be –0.087 eV. For the 4CP series eq 24 predicts χ_g = –0.050 eV.

The predicted values for χ_g of –0.087 and –0.050 eV for the resonance stabilization of the pz- and 4CP-bridged dimer series are in quite reasonable agreement with the observed average values of –0.081 and –0.021 eV obtained from the electrochemical studies

(50) (a) Zwickel, A. M.; Creutz, C. *Inorg. Chem.* **1971**, *10*, 2395–2399. (b) Creutz, C.; Chou, M. H. *Inorg. Chem.* **1987**, *26*, 2995–3000.
(51) Hupp, J. T. *J. Am. Chem. Soc.* **1990**, *112*, 1563–1565.
(52) Bertrand, P. *Chem. Phys. Lett.* **1987**, *140*, 57–63.
(53) We assume an additive contribution of 0.217 eV in all cases due to spin–orbit coupling effects; see ref 52.
(54) Kober, E. M.; Goldsby, K. A.; Narayana, D. N. S.; Meyer, T. J. *J. Am. Chem. Soc.* **1983**, *105*, 4303–4309.

Table VIII. Calculated[a] Parameters for the Symmetrical pz-Bridged Series $(L(NH_3)_4Ru)_2pz^{5+}$

L	S	β	Δ	ρ^a	ρ^*	a	b	μ_{th}[b]	μ_{spec}[b]	α
					trans-L					
(1) 3,5-Me_2py	0	−0.228	0.230	0.616	0.616	0.85	0.53	3.04	0.762	0.115
	0.2	−0.209	0.187	0.616	0.727	0.78	0.48	3.22	0.762	0.115
	0.35	−0.186	0.153	0.616	0.796	0.74	0.46	3.44	0.762	0.115
(2) py	0	−0.183	0.368	0.413	0.413	0.92	0.38	2.40	1.02	0.155
	0.2	−0.166	0.310	0.413	0.565	0.87	0.36	2.75	1.02	0.155
	0.35	−0.147	0.259	0.412	0.666	0.83	0.34	3.07	1.02	0.155
(3) 3-Fpy	0.2	−0.202	0.218	0.566	0.688	0.80	0.46	3.13	1.30	0.197
(4) 3-Clpy	0.2	−0.207	0.207	0.583	0.702	0.80	0.47	3.16	0.90	0.137
(5) 2,6-Me_2pz	0.2	−0.165	0.306	0.413	0.566	0.87	0.36	2.75	0.70	0.106
(6) bpy	0.2	−0.182	0.432	0.346	0.511	0.90	0.31	2.53	0.53	0.081
					cis-L					
(1) py	0	−0.211	0.328	0.490	0.490	0.90	0.44	2.69	0.99	0.150
	0.2	−0.192	0.272	0.490	0.628	0.84	0.41	2.97	0.99	0.150
	0.35	−0.170	0.225	0.490	0.717	0.79	0.39	3.24	0.99	0.150
(2) 3-Fpy	0.2	−0.220	0.191	0.624	0.733	0.78	0.49	3.23	0.87	0.132
av[c]	0.2	−0.19	0.27	0.51	0.64	0.83	0.42	2.98	0.89	0.134

[a] Based on the assumptions that $n \cong m'$ (see text) and $E_1^0 \cong -12.0$ eV (see ref 61). [b] Units are electron angstroms. [c] Calculated for the $S = 0.2$ cases.

of the rhodium analogues discussed in an earlier section. In fact, given the approximations we have had to make and the very simplified nature of the Mulliken treatment relative to more modern and complete quantum descriptions of these systems,[4,14,55-61] we find the level of agreement between experiment and theory evidenced on this point to be remarkable.

Wave Function Coefficients. Given our estimated values for S and ρ, it is now possible for us to calculate the coefficients a, a^*, b, and b^* in the variational ground- and excited-state wave functions written in eq 5. For a and b, this is done by using the ratio $\rho = b/a$ and the normalization condition

$$a^2 + 2Sab + b^2 = 1 \tag{25}$$

For a^* and b^* we must first consider the excited-state ratio $\rho^* = b^*/a^*$. In a derivation analogous to the one leading up to eq 16 it can be shown that the excited-state ratio is

$$\rho^* = \left[\frac{E_2^0\sigma - (E_1^0 + E_2^0)/2 + SH - R}{E_1^0\sigma - (E_1^0 + E_2^0)/2 + SH - R}\right]^{1/2} = \left[\frac{\Delta + 2(S(\beta_1 - S\Delta) - R)}{-\Delta + 2(S\beta_1 - R)}\right]^{1/2} \tag{26}$$

Once again, in the $S \cong 0$ limit we find $\rho^* = \sqrt{n}$. This expression in conjunction with the excited-state normalization condition

$$(a^*)^2 - 2Sa^*b^* + (b^*)^2 = 1 \tag{27}$$

allows us to calculate the excited-state coefficients.

The values of ρ, ρ^*, a and b are listed in Tables VIII and IX for the symmetrical dimers where we have used the assumption that $n \cong m'$ in our evaluation of R (see eq 15). For the pz-bridged series we obtain average, ρ, a, and b values of 0.51, 0.83, and 0.42, respectively. For 4CP the average ρ, a, and b are 0.24, 0.94, and 0.23. If the true value of n lies closer to the average of m and m' than to the least lower bound of m' itself (used in the calculations for Tables VIII and IX), then the pz-bridged average values become 0.76, 0.73, and 0.55. The 4CP values become $\rho = 0.315$, $a = 0.92$, and $b = 0.29$.

Electronic Coupling and Transition Dipole Calculations. Mulliken gives the following formula for the expected transition dipole of a charge-transfer absorption band:[8]

$$\mu_{theor} = \int \Psi_e \mu_{op} \Psi_g \, d\tau = [a^*b(\mu_2^0 - \mu_1^0) + (aa^* - bb^*)(\mu_{12} - S\mu_1^0)] \tag{28}$$

where μ_{op} is the transition dipole-moment operator, the difference $\mu_2^0 - \mu_1^0$ represents the change in dipole moment upon going from Ψ_1^0 to Ψ_2^0, and the second difference, $\mu_{12} - S\mu_1^0$, arises due to the dipole generated when a charge $-eS$ is transferred from the donor molecule to the average position of the overlap charge. This expression is analogous to the equation from Murrell's treatment which we have listed as eq 2a in the introduction section. Mulliken offered the following simplification of (28):

$$\mu_{theor} = a^*b(\bar{r}_2 - \bar{r}_1) + (aa^* - bb^*)S(\bar{r}_2 - \bar{r}_{12}) \tag{29}$$

where $\bar{r}_1$ and $\bar{r}_2$ represent the average position of the exchanging electron when completely localized on either the donor or the acceptor and $\bar{r}_{12}$ is the average postion of the overlap population. If we take the first difference as simply being the metal–metal separation d and the second difference as half of this, then (29) simplifies to

$$\mu_{theor} = d[a^*b + (S/2)(aa^* - bb^*)] \tag{30}$$

In the limit of small S and $a^* \cong 1$, eq 30 reduces to eq 2b.

In Tables VIII and IX we have listed the values obtained for μ_{theor} using eq 30 and our calculated values for a, a^*, b, and b^*. The spectroscopic value is defined by

$$\mu_{spec} = (0.02)\left[\frac{\epsilon_{max}\Delta\nu_{1/2}}{\nu_{max}}\right] \tag{31}$$

We also list the values of α calculated from the spectroscopic transition dipole using eq 3. From the tables we see that calculated transition dipoles based on the above assumptions considerably exceed the spectroscopic values. In the pyrazine case, the average ratio of μ_{theor}/μ_{spec} is 3.6. For 4CP the average is 4.6. Similar disagreement obtains if we compare the wave function coefficient b obtained from our electrochemical analysis and the coefficient α calculated from the experimental transition dipole and eq 3.

(55) (a) Zhang, L.; Ko, J.; Ondrechen, M. J. *J. Phys. Chem.* **1989**, *93*, 3030–3034. (b) Zhang, L.; Ko, J.; Ondrechen, M. J. *J. Am. Chem. Soc.* **1987**, *109*, 1666–1671. (c) Ondrechen, M. J.; Ko, J.; Zhang, L. *J. Am. Chem. Soc.* **1987**, *109*, 1672–1676.
(56) (a) Piepho, S. B.; Krauz, E. R.; Schatz, P. N. *J. Am. Chem. Soc.* **1978**, *100*, 2996–3005. (b) Neuenschwander, K.; Piepho, S. B.; Schatz, P. N. *J. Am. Chem. Soc.* **1985**, *107*, 7862–7869. (c) Prassides, K.; Schatz, P. *J. Phys. Chem.* **1989**, *93*, 83–89.
(57) (a) Piepho, S. B. *J. Am. Chem. Soc.* **1988**, *110*, 6319–6326. (b) Piepho, S. B. *J. Am. Chem. Soc.* **1990**, *112*, 4197–4206.
(58) (a) Larsson, S. *Chem. Phys. Lett.* **1982**, *90*, 136–139. (b) Broo, A.; Larsson, S. *Chem. Phys.* **1992**, *161*, 363–378.
(59) (a) Tanner, M.; Ludi, A. *Inorg. Chem.* **1981**, *20*, 2348–2350. (b) Joss, S.; Burgi, H. B.; Ludi, A. *Inorg. Chem.* **1985**, *24*, 949–954.
(60) Marcus, R. A. *J. Phys. Chem.* **1992**, *96*, 1753–1757.
(61) Lauher, J. W. *Inorg. Chim. Acta* **1980**, *39*, 119–123.
(62) We note that eq 30 already reflects the fact that less than a full electron is transferred in the transition. This is denoted by the presence of a,a^* and b,b^* in the equation.

Table IX. Calculated[a] Parameters for the Symmetrical 4CP-Bridged Series *trans*-$(L(NH_3)_4Ru)_2 4CP^{5+}$

L	S	β	Δ	ρ^a	ρ^*	a	b	μ_{th}[b]	μ_{spec}[b]	α
(1) 3,5-Me_2py	0	–0.203	0.905	0.214	0.214	0.98	0.21	1.90	0.505	0.056
	0.14	–0.194	0.839	0.214	0.344	0.95	0.20	2.44	0.505	0.056
	0.20	–0.188	0.803	0.214	0.397	0.94	0.20	2.67	0.505	0.056
(2) py	0	–0.216	0.889	0.230	0.230	0.97	0.23	2.04	0.619	0.069
	0.14	–0.206	0.822	0.230	0.358	0.95	0.22	2.55	0.619	0.069
	0.20	–0.200	0.785	0.230	0.411	0.93	0.22	2.78	0.619	0.069
(3) 4-Brpy	0.14	–0.231	0.763	0.270	0.395	0.93	0.25	2.82	0.667	0.074
(4) 4-Clpy	0.14	–0.244	0.754	0.286	0.409	0.93	0.27	2.92	0.619	0.068
(5) 3-Clpy	0.14	–0.067	0.936	0.071	0.208	0.99	0.07	1.28	0.526	0.058
(6) 3-Fpy	0.14	–0.215	0.805	0.243	0.371	0.94	0.23	2.65	0.487	0.054
(7) 2,6-Me_2pz	0.14	–0.204	0.914	0.207	0.338	0.95	0.20	2.39	0.355	0.039
av[c]	0.14	–0.22	0.82	0.24	0.37	0.94	0.23	2.63	0.542	0.060

[a] Based on the assumptions that $n \cong m'$ (see text) and $E_1^0 \cong -12.0$ eV (see ref 61). [b] Units are electron angstroms. [c] Average calculated for the $S = 0.14$ cases, omitting the data for 3-Clpy.

For pz as bridge, we find an average value of 3.3 for the b/α ratio. For 4CP the average is 3.5.

These results indicate that the discrepancy between the wave function coefficients arrived at *via* the electrochemical/Mulliken approach outlined here and the spectroscopic Murrell/Hush formalism has its origins in the difference between the experimental transition moment and the one which would be consistent with theory based on the magnitudes of ρ, ρ^*, and S. Recent work by OH and Boxer using Stark effect spectroscopy has shown that the actual charge-transfer distance in intervalence-transfer transitions may in fact be substantially less than the simple geometric distance between the metal sites.[22] Hupp has pointed out the possible significance of this with regards to reconciling optically and electrochemically derived estimates of the electronic coupling in mixed-valence dimers.[20] In the case of the present systems, however, we would have to divide the distance parameter d in eq 30 by 3.6 and 4.6 in order to bring the observed and calculated transition moments into agreement for the pz- and 4CP-bridged series, respectively. In order to bring the wave function coefficient b into agreement with the optically-derived α value from eq 3, the geometric distance would have to be divided by factors of 3.3 and 3.5. Some diminution of the effective distance between the charge centroids would be predicted given the participation of the bridging ligand π^* levels in the HOMO's of the zero-order states (see Figure 7 and the discussion preceding eq 19), but this effect is at least approximately accounted for by the second term in eqs 28–30. Distance corrections by factors of as much as 3 or more are not obviously explicable to us.

In light of the above, we are lead to question the validity of eqs 28–30 when applied to relatively strongly coupled mixed-valence systems such as those reported on here. This comes as no surprise in the case of the pz-bridged series given that it has been widely recognized that coupling in the Creutz–Taube ion is strong enough to require a delocalized MO treatment for an accurate description of its electronic structure.[2,55–57,58b,59,61,63–65] It is surprising, however, that the same level of discrepancy persists even for the 4-cyanopyridine dimers.

Equations 28–30 are based on a simple one-electron model for a formal bonding-to-antibonding transition. Detailed molecular orbital analyses of the electronic structure of these systems, however, indicate that the intervalence transfer transition is substantially bonding-to-nonbonding in character.[50,55b,57,61] Vibronic effects are also thought to be very important in determining the details of the IT band shapes and intensities in these complexes.[55–57] It may simply be that eqs 28–30, and hence eq 3, are outside of their range of applicability even in systems as strongly coupled as the 4-cyanopyridine dimers studied here.

The electrochemical/Mulliken approach outlined in this paper clearly rests on a highly simplified, one-electron quantum description of the system and a relatively large set of assumptions regarding the interpretation of the observed electrochemical potential shifts. A major strength, however, is that the range of applicability with regards to the overlap integral S and the mixing parameter ρ is not as highly restricted as it is in the case of the spectroscopic/Murrell–Hush formalism. Independent assessments of the degree of coupling in these systems such as, for example, the ESR measurements reported by Westmoreland *et al.*[18] and the resonance Raman data discussed by Mines *et al.*[19] should prove to be very helpful in sorting out the ranges of validity and usefulness for the two approaches.

An Alternative Measure of Delocalization Based on Bandwidth. Figure 5 illustrates the effects of the various synthetic manipulations on the intervalence-transfer absorption bandwidth and the electrochemical peak splitting $\Delta E_{1/2}$ for the pz-bridged complexes (no such pronounced trends are evident in the 4CP-bridged dimers). The curves show us that the electronic structure can be tuned from delocalized, the Creutz–Taube ion case where $\Delta\nu_{1/2} = 0.184$ eV, to localized, $\Delta\nu_{1/2} \cong 0.5$ eV, either by placing a single π-back-bonding ligand on one side of the Creutz–Taube ion and thereby imparting a redox asymmetry to the dimer as well as decreasing π-back-bonding to the bridge or by symmetrically substituting the dimer in such a way that only π-back-bonding to the bridge is affected.

We can use the bandwidth effects of these procedures to create a provisional "degree of delocalization" scale. We will postulate that a bandwidth of 0.184 eV (the experimental value for the Creutz–Taube ion) represents a degree of delocalization, ω, of 1.0. We further postulate that a bandwidth on the order of 0.558 eV, as is observed for strongly valence-trapped Callahan dimer,[66] represents an ω value of 0.0. These two assumed extrema allow us to place the pz-bridged dimers on the ω scale according to their observed bandwidths.

Figure 9 shows a plot of ω for each dimer vs the potential of the appropriate $L(NH_3)_4Rupz^{2+/3+}$ monomer couple (presumably a reasonable measure of the strength of the perturbation being applied). It is clear from the figure that asymmetrical substitution leads to a faster loss of delocalization through most of the potential range. The main point of interest is that both plots, and especially the one for the symmetrical dimers (the open points), indicate a fairly abrupt change in slope at a certain point. The symmetrical dimer data clearly indicate a rapid change from mostly delocalized to mostly localized at a monomer potential of approximately 0.38 V. This trend falls in line with the recent prediction made by

(63) Hush, N. S. In *Mixed-Valence Compounds*; Brown, D. B., Ed.; NATO Adv. Study Ins. Ser. 58; D. Reidel: Boston, MA, 1980, pp 151–188.
(64) Beattie, J. K.; Hush, N. S.; Taylor, P. R. *Inorg. Chem.* **1976**, *15*, 992–993.
(65) Wong, K. Y.; Schatz, P. N.; Piepho, S. B. *J. Am. Chem. Soc.* **1979**, *101*, 2793–2799.
(66) Callahan, R. W.; Keene, F. R.; Meyer, T. J.; Salmon, D. J. *J. Am. Chem. Soc.* **1977**, *99*, 1064.

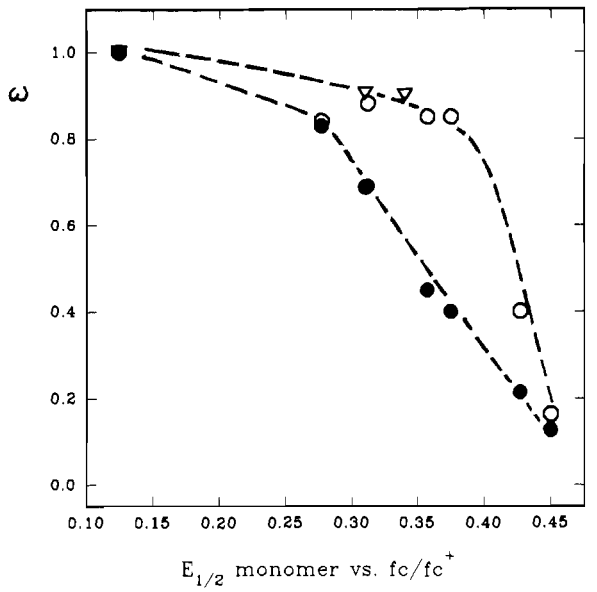

Figure 9. Variation in the degree of delocalization parameter ω (calculated from the bandwidth data in Tables III and IV) with stronger and stronger applied perturbation (as indicated here by the potential of the appropriate monomer compound selected from Table I): Filled circles, *trans*-$L(NH_3)_4Ru_b$–pz–$Ru_a(NH_3)_5^{5+}$; open circles, (*trans*-$L(NH_3)_4Ru)_2pz^{5+}$; open triangles, (*cis*-$L(NH_3)_4Ru)_2pz^{5+}$.

Broo and Larsson that the Robin and Day class III/class II transition as a function of dimeric structure should by fairly sharp.[58b] The same trend is not clearly present in the *m'*-derived measures of delocalization listed in Table VIII, although it may be showing up in the significantly smaller value of ρ obtained for the triammine–bpy species. Importantly, inspection of Table VII where we list the χ_g values arising from the resonance interaction in the symmetrical pz-bridged systems reveals no such pronounced transition. Whether this reflects a real difference between the thermodynamic and the spectroscopic consequences of the change in electronic structure or simply the noise level in our electrochemical χ_g measurements is unclear.

Concluding Remarks. The Mulliken model for donor–acceptor interactions provides a simple and useful theoretical framework for understanding certain broad aspects of the electronic coupling in mixed-valence binuclear complexes. Although it is only a one-electron treatment of the problem and is by no means a full quantum description of the system,[4,14,55–61] we find that by extending the theory to include electrochemical potential shift data resulting from synthetic manipulations we are able to gain valuable insight into the magnitude of the quantum coupling and the resonance delocalization energy in simple dimeric systems. Our results indicate that the extent of wave function mixing in these systems as measured by the wave function coefficient *b* exceeds the estimate of α arrived at *via* eq 3 and spectroscopically-based input data by a factor of at least 3.5 or so. The relative ordering of the coupling in the pz- and 4CP-bridged dimers, however, remains in good qualitative agreement. Comparing the average coupling obtained as a function of bridging ligand, we find $b(4CP)/b(pz) = 0.55$ and $\alpha(4CP)/\alpha(pz) = 0.45$.

Acknowledgment. The early phases of this work were supported by a Type B grant from the Petroleum Research Fund, administered by the American Chemical Society. We wish to acknowledge recent support from the National Science Foundation RUI program under Grant No. Che-9200446. We also wish to gratefully acknowledge the loan of the ruthenium used in this study from the Johnson Matthey Platinum Group Metals loan program. J.C.C. thanks Prof. John F. Endicott of Wayne State University for his thoughtful comments. Last, we thank Prof. Ray Trautman of San Francisco State University for running the FTIR spectra for us.

Appendix. Application to the Wolfsberg–Helmholz Approximation

A frequently employed approximation in the calculation of molecular orbitals from atomic orbital basis sets is the Wolfsberg–Helmholz relation, which allows for the convenient computation of off-diagonal matrix elements,

$$H_{ij} \cong K_{ij}S_{ij}(H_{ii} + H_{jj})/2 \qquad \text{(A1)}$$

where K_{ij} is an empirically chosen parameter.[67] For atomic orbitals, the optimum value for the adjustable paramer K is typically found to be about 1.75. In principle, it should be possible to use the data and parameters we have generated in this study to solve for the effective K_{ij} values that would apply to a *molecular* analog of eq 32,

$$\mathbf{H} \cong K_{12}\mathbf{S}(E_1^\circ + E_2^\circ)/2 \qquad \text{(A2)}$$

Substituting eq 33 into the definition of β allows us to write

$$K = \frac{2(\beta_1 + \mathbf{S}E_1^\circ)}{\mathbf{S}(2E_1^\circ + \Delta)} \qquad \text{(A3)}$$

For the symmetrical pz-bridged series at an assumed **S** value of 0.2 we find $K_{12} = 1.09$. For the 4CP series at $\mathbf{S} = 0.14$ we find $K_{12} = 1.16$. We note that these values do not change substantially depending on whether we use m' or $m_{av} = (m + m')/2$ in our calculation of β_1 and Δ. Neither is there a very strong dependence on our choice of **S**. It is interesting that the two values are as close as they are. In a theoretical study of linear-chain phthalocyanine-based complexes Pietro, Marks, and Ratner arrived at a K_{12} value of 0.5 for a molecular analog of eq 32.[68] Thus, there is some supporting precedent for a diminished magnitude of K in the molecular *vs* atomic application of the Wolsfberg–Helmholz relationship.

(67) (a) Mulliken, R. S. *J. Chim. Phys.* **1949**, *46*, 497, 675. (b) Wolfsberg, M.; Helmholz, L. *J. Chem. Phys.* **1952**, 837–843. (c) Hoffmann, R. I. *J. Chem. Phys.* **1963**, *39*, 1397–1412; **1964**, *40*, 2474, 2745. (d) Cusachs, L. C.; Cusachs, B. B. *J. Phys. Chem.* **1967**, *71*, 1060–1073.

(68) Pietro, W. J.; Marks, T. J.; Ratner, M. A. *J. Am. Chem. Soc.* **1985**, *107*, 5386–5391.